

Restricted

Contract Report

**The Development of
Structural Design Models
for Foamed Bitumen
Treated Pavement Layers**

Author:

F M Long

PREPARED FOR:

SABITA Ltd
PO Box 6946
ROGGEBAAI
8012

PROJECT MANAGER:

Asphalt Academy
PO Box 395
PRETORIA
0001

PREPARED BY:

CSIR Transportek
PO Box 395
PRETORIA
0001
Tel: +27 12 841 2905
Fax+27 12 841 3232

DOCUMENT RETRIEVAL PAGE			Report No: Report CR-2001/76	
Title: The Development of Structural Design Models for Foamed Bitumen Treated Layers				
Authors: F M Long				
Client: SABITA	Client Reference No:	Date: December 2001	Distribution: Restricted	
Project No: TIJ53	OE2: 9431: Transport Infrastructure		ISBN:	
Abstract: <p>This report describes the development of structural design models for foamed bitumen treated pavement layers. The structural design model is a mechanistic-empirical design procedure that will ultimately be incorporated into the South African Mechanistic-Empirical Design Method.</p> <p>Laboratory testing showed that the addition of cement adds flexural and compressive strength, and therefore permanent deformation resistance, to the material, while foamed bitumen adds flexibility, and therefore fatigue resistance.</p> <p>The structural design models were developed from Heavy Vehicle Simulator (HVS) and laboratory testing. The transfer function for permanent deformation was developed in the laboratory and calibrated using the HVS results. This function relates the structural capacity of the pavement, in terms of load repetitions, to the stress ratio determined from multi-layer linear elastic pavement analyses. The effective fatigue transfer function was developed from HVS data, and relates the effective fatigue life to the strain ratio. The strain ratio is determined from the ratio of the strain at the bottom of the foamed bitumen treated layer in a mechanistic analysis to the strain-at-break, which is the maximum strain at the moment of crack initiation for a flexural beam test.</p> <p>The report discusses the laboratory and HVS data used to develop the transfer functions.</p>				
Keywords: deep in situ recycling, foamed bitumen permanent deformation model, elastic stiffness model, mechanistic-empirical design procedure, Heavy Vehicle Simulator				
Proposals for implementation: Report supplied to client for implementation.				
Related documents: <ol style="list-style-type: none"> 1. Long, F.M. and H.L.Theyse, <i>Laboratory Testing for the HVS Sections on Road P243/1</i>, Transportek, CSIR, Contract Report CR-2001/22, 2001. 2. Steyn, W.J.vdM., <i>Level one data analysis of HVS tests on Foam Treated Gravel and Emulsion Treated Gravel on Road P243-1: 80 kN and 100 kN test sections</i>, Transportek, CSIR, Contract Report CR-2001/5, 2001. 3. Mancotywa, W.S., <i>First Level Analysis Report: 2nd phase HVS Testing of the Emulsion Treated Gravel and Foam Treated Gravel Base Sections on Road P243/1 near Vereeniging</i>, Transportek, CSIR, Contract Report CR-2001/53, 2001. 4. Robroch, S., <i>Laboratory Testing on Foamed Bitumen and Cement Treated Materials from the HVS Test Sections on Road P243/1</i>, Transportek, CSIR, Contract Report, CR-2001/69, 2001. 				
Signatures:				
K Wolhuter Language Editor	H Theyse Technical Reviewer	BMJA Verhaeghe Programme Manager	S Roets Info Centre	PJ Hendricks Division Director
NOTE: This document is confidential to TRANSPORTEK and may only be distributed with the written permission of the Director or his nominee.				

EXECUTIVE SUMMARY

This report describes the development of structural design and performance models for foamed bitumen treated materials. The purpose of developing these models is to incorporate them into the South African Mechanistic-Empirical Design Method. To date no mechanistic-empirical design models have been available for foamed bitumen treated materials.

The development of the design models is based on data from laboratory and Heavy Vehicle Simulator (HVS) testing. The HVS tests consisted of two foamed bitumen treated test sections constructed using deep in situ recycling. The milled material consisted of the cement treated ferricrete base with the old multi seal surfacings and some of the untreated ferricrete subbase. This material was treated with 2 percent cement and 1.8 percent foamed bitumen. Two wheel loads were used, 40 kN and 80 kN. The 40 kN HVS wheel load corresponds to an E80 standard axle. Various instruments were used during the tests including Multi-Depth Deflectometers (MDD) to measure the in-depth elastic deflections and permanent deformation.

Two distress mechanisms were observed on the HVS test sections, effective fatigue and permanent deformation. The test sections showed more fatigue distress than permanent deformation distress.

- **Effective fatigue:** Back-calculated foamed bitumen base layer stiffnesses showed that the stiffness initially rapidly reduced and then reduced more gradually until a constant stiffness was reached. Regardless of the load, the same constant stiffness value was reached. This constant stiffness indicates the layer has reached an equivalent granular state. The term “equivalent granular state” is used to describe the loss in resilient modulus (stiffness) of the material and is comparable to granular materials only in the stiffness and not in the physical composition of the materials. The term does not imply that the material is in a loose condition consisting of individual particles. The number of load repetitions to reach this equivalent granular state is defined as the effective fatigue life.
- **Permanent deformation:** The majority of the permanent deformation in the pavement came from the foamed bitumen base layer, although the amount of permanent deformation was small. The permanent deformation increased fairly rapidly in the beginning while the pavement was bedding in, and then continued at a more gradual rate.

The laboratory program included the following tests:

- unconfined compressive strength tests (UCS);
- flexural beam fatigue tests to determine the strain-at-break;
- static triaxial tests to determine the static strength parameters (cohesion and friction angle), and
- dynamic triaxial tests to determine the resilient modulus and permanent deformation response.

Tests were run with 1 and 2 percent cement, and a range of foamed bitumen contents.

The laboratory tests highlighted the effect of cement and foamed bitumen treatment, and the ratio of the cement to foamed bitumen contents, on the strength and flexibility of an untreated material.

- **Flexibility:** The addition of foamed bitumen, or a decrease in the cement to foamed bitumen content ratio, increases the flexibility, and therefore the fatigue resistance of the material. The strain-at-break value from the flexural beam tests showed that the higher the binder content or lower the cement to binder content ratio, the higher the strain-at-break value and therefore the higher the fatigue resistance. However, if insufficient foamed bitumen is added, there is no increase in the flexibility of the mix.
- **Compressive and flexural strength:** The addition of cement or an increase in the cement to foamed bitumen content ratio increases both the compressive and flexural strength of the foamed bitumen treated materials. An increase in the foamed bitumen content or a decrease in the cement to binder content ratio decreases the compressive and flexural strength of cement treated materials. An increase in the compressive strength results in an increased permanent deformation resistance.

To optimise the material behaviour for compressive and flexural strength, and flexibility, it is important to balance the foamed bitumen and cement contents. The optimum balance will depend on the untreated material and the desired pavement behaviour.

The development of the mechanistic-empirical structural design procedure is based on examining the material behaviour and distress mechanisms in the pavement from the HVS tests, and in the laboratory. In the design models, this behaviour is related to engineering parameters determined from mechanistic analyses of the pavement structure. The predicted structural capacity determined from the models is also dependant on the level of reliability assumed for the road category.

A structural design model for effective fatigue was developed using the elastic stiffness data from the HVS. The model determines the number of repetitions to the equivalent granular state as a function of the strain ratio. The strain ratio is the ratio of the tensile strain at the bottom of the pavement layer to the strain-at-break from the flexural beam test. The tensile strain in the pavement is calculated using a multi-layer linear elastic analysis of the pavement.

The foamed bitumen layer in the HVS test sections had 2 percent cement and 1.8 percent foamed bitumen. The effect of different cement or foamed bitumen contents is accounted for with the strain-at-break value and the corresponding strain ratio. Increasing the binder content results in an increased strain-at-break and therefore increased effective fatigue life. This model is similar to the effective fatigue model for cement treated materials given in TRH4. However, the foamed bitumen materials have a higher strain-at-break, which results in a larger effective fatigue life than the cemented materials.

The permanent deformation model was developed from dynamic triaxial laboratory tests, and calibrated using the HVS data. The laboratory model determines the repetitions to a level of plastic strain as a function of the relative density, stress ratio and the ratio of the cement to foamed bitumen contents. The stress ratio is the ratio of the stress in the material to the maximum allowable stress. The in-depth permanent deformations measured by the MDDs were used to fit a model that determines the repetitions to a level of plastic strain as a function of the stress ratio in the pavement calculated from multi-layer linear elastic analyses of the HVS pavement structures.

Comparison of the laboratory and HVS permanent deformation models, using the relative density of the HVS test section, a range of plastic strains, the stress ratios determined for the HVS test sections, and the cement to foamed bitumen content ratio showed that the laboratory model predicts more permanent deformation resistance than the HVS model. The material in the laboratory tests was new and was not subjected to any damage prior to testing. The boundary condition of the HVS tests are closer to the expected boundary conditions in the field. For these reasons it is likely that the HVS model is closer to field results than the laboratory model and it is reasonable to shift the laboratory model predictions to be in closer agreement with the HVS model predictions. A constant shift factor brings the two models into closer agreement. By calibrating the laboratory model with the HVS model, the model is applicable to a wider range of cement and foamed bitumen contents than just the combination used in the HVS test sections.

For applicability to a wider range of cement and foamed bitumen contents, the permanent deformation structural design model integrates the laboratory model and the shift factor from the HVS model.

Damage exponents were developed for permanent deformation and effective fatigue from the HVS data to determine the relative damage caused by a higher load. The damage exponents for effective fatigue and permanent deformation are approximately 5.6 and 2.4, respectively. These damage exponents are applicable to the pavement structures, the materials and the environmental conditions of the HVS test sections. These exponents show that the effective fatigue response is more load sensitive than the permanent deformation response.

TABLE OF CONTENTS

EXECUTIVE SUMMARY..... i

LIST OF TABLES..... iii

LIST OF FIGURES..... iv

ACKNOWLEDGEMENTS v

1. INTRODUCTION..... 1

1.1. Background 1

1.2. Objectives and Deliverables..... 1

2. HEAVY VEHICLE SIMULATOR (HVS) TESTING 3

2.1. Materials and Construction..... 3

2.2. Loading Sequence 4

2.3. Instrumentation..... 5

2.4. Results..... 6

2.4.1 Surface Permanent Deformation 6

2.4.2 In-depth Permanent Deformation..... 7

2.4.3 Elastic Deflections..... 8

2.4.4 Back-calculated Elastic Stiffness 9

2.5. Visual Observations 12

3. LABORATORY TESTING 14

3.1. Unconfined Compressive Strength (UCS) 14

3.2. Flexibility..... 15

3.3. Shear Strength 17

3.4. Elastic Stiffness (Resilient Modulus) 19

3.5. Permanent Deformation 20

3.6. Discussion 22

4. STRUCTURAL DESIGN AND PERFORMANCE MODELS 24

4.1. Design Philosophy..... 24

4.2. Permanent Deformation 24

4.2.1 Regression Model for In-depth MDD Permanent Deformation Data 24

4.2.2 Permanent Deformation Model from HVS Data..... 25

4.2.3 Mechanistic Pavement Analyses for Permanent Deformation..... 27

4.3. Development of Transfer Functions for Permanent Deformation 32

4.3.1 Transfer Function from HVS Data..... 32

4.3.2	Permanent Deformation Transfer Function.....	33
4.4.	Effective Fatigue.....	36
4.4.1	HVS Effective Fatigue Transfer Function.....	36
4.4.2	Mechanistic Pavement Analysis for Effective Fatigue	38
4.4.3	Effective Fatigue Transfer Function	38
4.4.4	Comparison of Effective Fatigue Life Transfer Functions for Foamed Bitumen and Cemented Materials	40
4.5.	Load Sensitivity and Damage Exponents	41
4.5.1	Permanent Deformation	41
4.5.2	Effective Fatigue	43
5.	CONCLUSIONS.....	44
6.	REFERENCES.....	46

LIST OF TABLES

Table 1. HVS Test Section Loading Sequence..... 5

Table 2. UCS Test Results 15

Table 3. Flexural Beam Test Results 16

Table 4. Ranges of Resilient Modulus Values 19

Table 5. Permanent Deformation Damage Exponents for Combinations of MDDs
and Test Sections 42

Table 6. Effective Fatigue Damage Exponents for Combinations of MDDs and Test Sections 43

LIST OF FIGURES

Figure 1. Grading of Milled, Untreated Ferricrete 3

Figure 2. HVS Test Section Pavement Structure..... 4

Figure 3. HVS Test Section Layout and Dimensions..... 6

Figure 4. Surface Permanent Deformation 7

Figure 5. In-depth Permanent Deformation for MDD8, Section 411A4 8

Figure 6. Elastic Surface Deflection Measured with the RSD..... 9

Figure 7. Elastic Surface Deflections Across Section 411A4 9

Figure 8. Back-calculated Base Layer Stiffnesses from MDD Measured Deflections 11

Figure 9. Crack Patterns on HVS Test Sections..... 13

Figure 10. Strain-at-break 16

Figure 11. Cohesion and Friction Angle from Static Triaxial Test..... 18

Figure 12. Structural Capacity Model from Laboratory Permanent Deformation Tests..... 22

Figure 13. Strength and Flexibility of Foamed Bitumen Treated Materials..... 23

Figure 14. Base Layer MDD Permanent Deformation Regression Model Fits 25

Figure 15. HVS Derived Permanent Deformation Model for Foamed Bitumen Treated Material..... 26

Figure 16. Maximum Stress Ratio..... 29

Figure 17. Location of Tyres in Analyses..... 30

Figure 18. Location of Maximum Stress Ratio 30

Figure 19. Recommended Locations to Calculate the Stress Ratio 31

Figure 20. Structural Capacity as a Function of Stress Ratio from HVS Data..... 33

Figure 21. Comparison of Laboratory and Permanent Deformation HVS Transfer Functions 34

Figure 22. Permanent Deformation Transfer Function 36

Figure 23. Effective Fatigue Life for Foamed Bitumen Treated Base Material..... 37

Figure 24. Effective Fatigue Life Transfer Function 39

Figure 25. Comparison of Foamed Bitumen and Cemented Materials Effective Fatigue Lives 41

ACKNOWLEDGEMENTS

The laboratory and HVS testing used to develop the structural design models was funded by the Gauteng Provincial Government, Department of Transport and Public Works, South Africa. The development of the design models for incorporation into the “Interim Guidelines for the Design and Use of Foamed Bitumen Treated Base Layers” is being funded by SABITA, and managed on their behalf by the Asphalt Academy.

Some of the laboratory testing and analyses discussed in this report were performed by Sietse Robroch, as part of his Masters degree thesis for the Delft University of Technology. His contributions are gratefully acknowledged.

A review committee consisting of Elzbieta Sadzik from Gautrans, Ian van Wijk from Africon, Kim Jenkins from the University of Stellenbosch, Dave Collings and Matthew Houston from AA Loudon and Partners, and Les Sampson from the Asphalt Academy reviewed this report. Their inputs were extremely valuable to the project and their comments have been incorporated.

1. INTRODUCTION

1.1. Background

The use of foamed bitumen in the construction of pavement layers is increasing both nationally and internationally. These materials are used as a method of cold treatment, and are particularly useful when used in conjunction with the Deep In Situ Recycling (DISR) technology. With the growing need to construct new roads for rural access in southern Africa and to rehabilitate existing roads, these materials are a viable option, because of the many advantages associated with their use, including:

- The ability to open the rehabilitated road to traffic immediately after construction, thereby eliminating the need to construct temporary detours and minimizing traffic disruption;
- Cheaper construction costs than standard methods of rehabilitation; and
- Lower quality aggregates can be effectively used in pavement layers when treated with foamed bitumen or bituminous emulsion.

Although foamed bitumen treated materials have been successfully used in South Africa for a number of years, the structural adequacy of these materials has not been proven and no guidelines for their use are available. Research is currently underway to assess their use in the road-building industry. This research includes laboratory testing, Heavy Vehicle Simulator (HVS) testing, and field trials.

1.2. Objectives and Deliverables

Although foamed bitumen and bituminous emulsion treated materials are currently being tested, this report only discusses the results from HVS and laboratory testing on foamed bitumen treated materials. These results are used to determine structural design and performance models for both effective fatigue and permanent deformation, for incorporation into the South African Mechanistic-Empirical Design Method. The design philosophy and the procedure followed to develop the models are discussed. The models are developed from the available HVS and laboratory test data. The HVS tests were performed on one material with one combination of cement and foamed bitumen contents. The laboratory tests were performed on the same material with a wider range of cement and foamed bitumen contents.

This report is the first deliverable in the preparation of the "Interim Guidelines for the Design and Use of Foamed Bitumen Treated Base Layers: Phase 2". The models

described in this report will be used in the structural design chapter of the interim guideline document and also used to develop the catalogue of pavement structures to be included in the guidelines.

2. HEAVY VEHICLE SIMULATOR (HVS) TESTING

The Heavy Vehicle Simulator (HVS) test sections were constructed on Road P243/1 between Vereeniging and Balfour in the Gauteng Province of South Africa. This chapter discusses the materials and construction of the test sections, and the test results.

2.1. Materials and Construction

The original pavement consisted of the surfacing, a cement stabilised ferricrete base layer, an untreated ferricrete subbase layer and a natural subgrade layer. The surfacing consisted of multiple seals. The pavement was recycled with a Wirtgen type recycling machine to a nominal depth of 250 mm. The recycled material therefore contained the milled surfacing and ferricrete from the base and subbase layers. A large quantity of this milled material was retained for laboratory testing. The optimum moisture content of the milled material is 12.5 percent, and maximum dry density is 1971 kg/m³. The grading of the milled material is shown in Figure 1. The grading is similar to that of a crushed stone material^{1,2}.

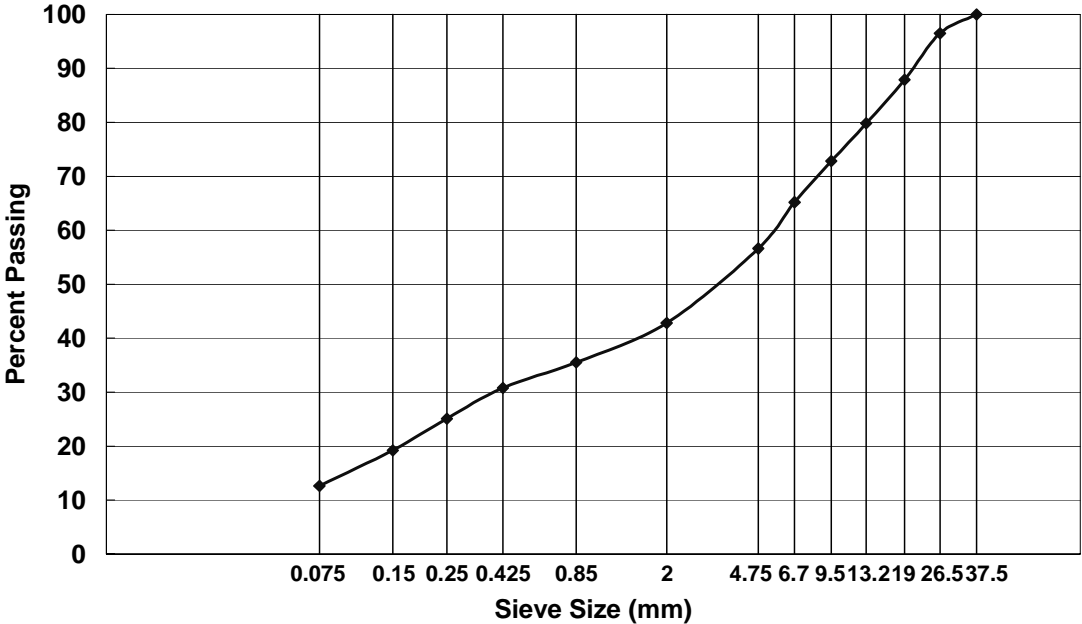


Figure 1. Grading of Milled, Untreated Ferricrete

The majority of the road was rehabilitated by treating the recycled material with foamed bitumen, and a 100 metre section was recycled with bituminous emulsion. The foamed

bitumen sections were treated with 1.8 percent residual foamed bitumen (80/100 pen) and 2 percent cement. A spring near the test sections resulted in high moisture contents, both before and after construction. Moisture contents of approximately 11.3 percent were measured in the base layer².

The structure of the rehabilitated pavements comprises of 25 mm asphalt concrete surfacing, 250 mm of foamed bitumen treated material, 250 mm untreated ferricrete subbase with a G6 classification, and the natural subgrade. This pavement structure is shown in Figure 2. The design thicknesses, and the actual base and surfacing thicknesses measured in test pits are shown. The actual thicknesses were measured at three locations.

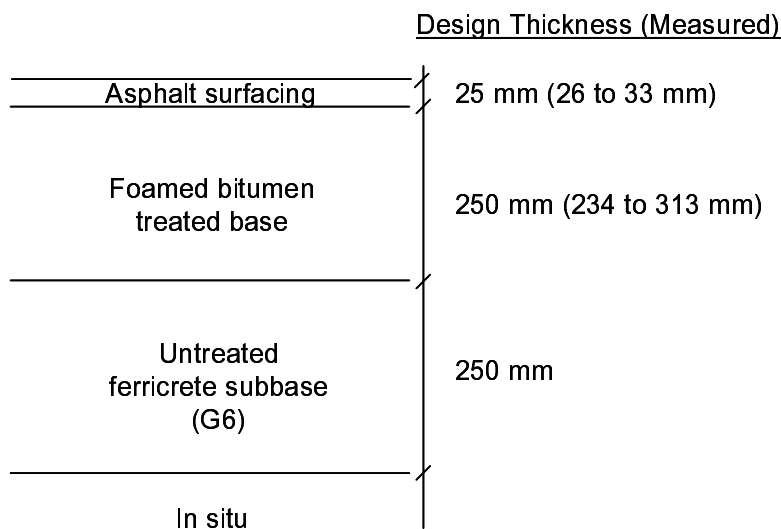


Figure 2. HVS Test Section Pavement Structure

Two HVS test sections were tested on each of the foamed bitumen and bituminous emulsion treated base pavements. The exact location of the test sections were selected from areas of fairly uniform falling weight deflectometer deflections. The foamed bitumen treated sections were designated 409A4/B4 and 411A4. The bituminous emulsion treated sections were designated 410A4/B4 and 412A4. The first level analyses of these HVS test sections are described by Steyn³ and Mancotywa⁴. The remainder of this report will discuss the foamed bitumen treated sections, 409A4/B4 and 411A4, only.

2.2. Loading Sequence

The HVS testing consisted of two phases, which are detailed in Table 1. In Phase 1, after the application of the 80 kN load repetitions (409A4), the HVS was moved to create

a new test section (409B4). This new 8 m test section consisted of 4 m of the previous test section, and 4 m of untrafficked pavement³. Once water was added, it was continuously applied during trafficking.

Table 1. HVS Test Section Loading Sequence

PHASE 1				
Test Sections	Repetitions	Load (kN)	Tyre Pressure (kPa)	Comments
409A4	307 224	80	800	
409B4	147 606	100	850	
	7 694	100	850	Water added
PHASE 2				
Test Sections	Repetitions	Load (kN)	Tyre Pressure (kPa)	Comments
411A4	958 714	40	620	
	340 883	80	800	
	14 048	80	800	Water added

2.3. Instrumentation

During the HVS tests, the pavement condition was assessed at regular intervals with measurements of the elastic deflection, permanent deformation, temperature and moisture conditions, and from visual observations. Various pavement response instruments were used including:

- multi-depth deflectometer (MDD);
- road surface deflectometer (RSD);
- falling weight deflectometer (FWD);
- laser profilometer;
- straight edge;
- thermocouples; and
- dynamic cone penetrometer (DCP).

The MDDs were installed at the following depths in the pavement structure: 25 mm, 275 mm, 450 mm, 650 mm, and 850 mm. Two MDDs were installed in Section 409A4, and three MDDs in Section 411A4. For reference, the 8 m HVS test section was labelled every half a metre, from 0 to 16. The MDD number is a reference to the location on the test section, i.e., MDD4 is at point 4, as shown in Figure 3.

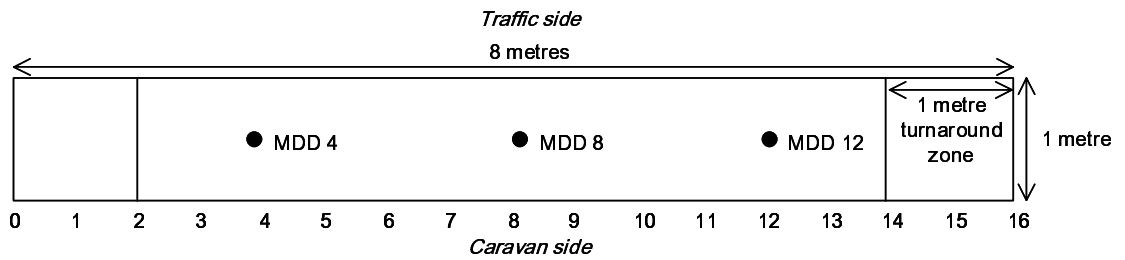


Figure 3. HVS Test Section Layout and Dimensions

2.4. Results

The only results from the HVS tests discussed in this report are those that either add insight into the test section behaviour, or are used to develop the structural design and performance models. All the data from the test sections are presented and discussed by Steyn³ and Mancotywa⁴.

2.4.1 Surface Permanent Deformation

Surface rutting was measured with a straight edge. Figure 4 shows the straight edge measured average surface rut. The data in the early stages of a test are fairly variable. This is because of the coarseness of the measurement device, and the small amounts of rutting experienced. The measurements below 2 mm of rutting are therefore fairly inaccurate.

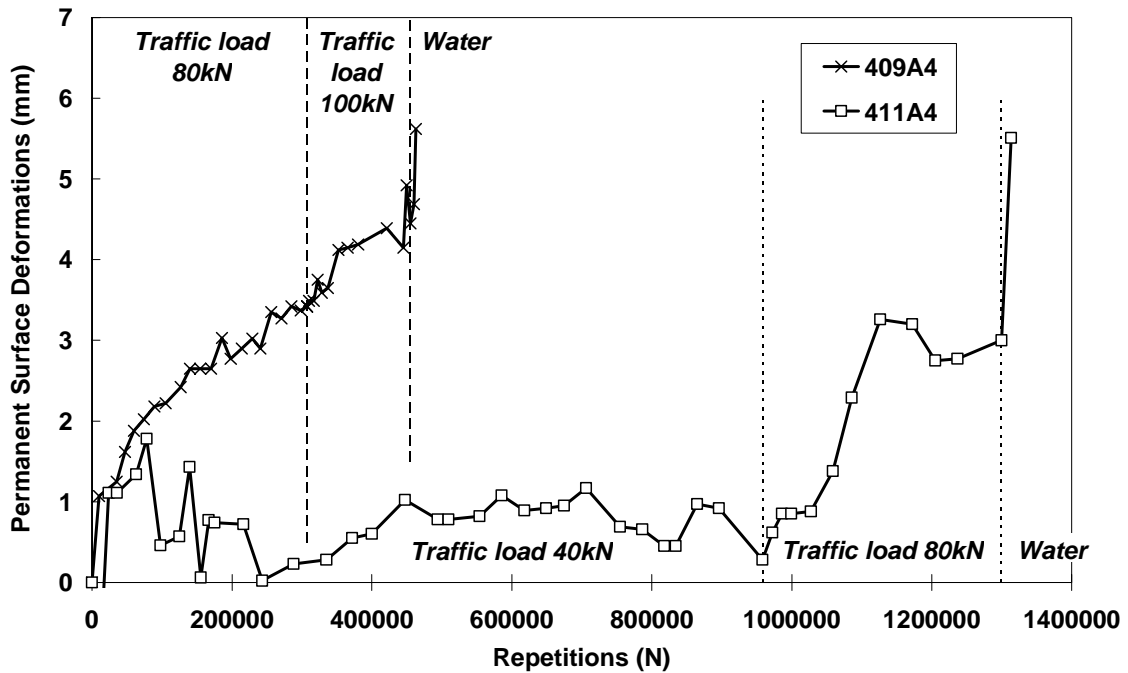


Figure 4. Surface Permanent Deformation

As expected, the higher loads resulted in a higher rate of rutting and once water was added to the section, the rutting increased dramatically. Although significant rutting was only experienced after the addition of water, known as moisture accelerated distress (MAD), there was still relatively little permanent deformation. The rut was formed by fines being pumped to the sides of the test section.

2.4.2 In-depth Permanent Deformation

The accumulation of in-depth permanent deformation was measured with the MDD. Figure 5 shows an example of the results from MDD8 on Section 411A4. A considerable amount of rutting occurred in the layers underlying the foamed bitumen base under the higher wheel load. The difference between the deformation of MDDs at the top and bottom of the layer can be subtracted to obtain the deformation for that layer, as shown in Figure 5. This in-depth permanent deformation data for the base layer is used to develop the structural design models.

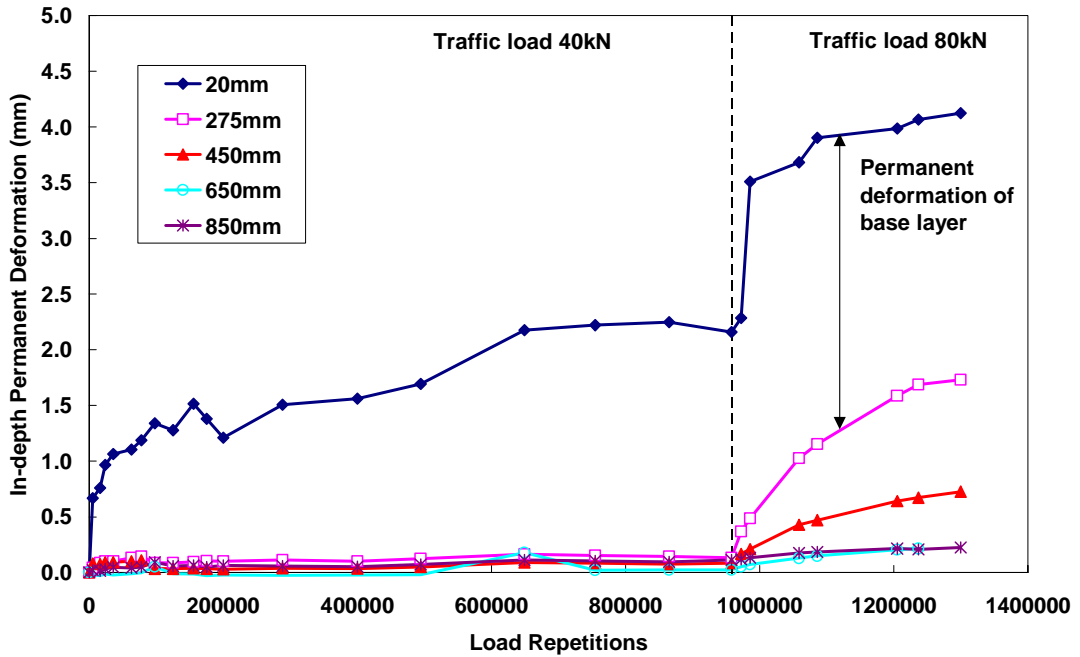


Figure 5. In-depth Permanent Deformation for MDD8, Section 411A4

2.4.3 Elastic Deflections

The elastic surface deflections measured with the RSD are shown in Figure 6. A fairly wide range of deflections was measured along the test section. The values shown in Figure 6 are the averages for the data measured along the centreline. As an example of the variation across a test section, all the RSD data points are shown in Figure 7 for Section 411A4. The data points from the first four metres of the test section (points 0 to 8) are shown as solid diamonds and, for the second four metres (point 8 to 16), as open squares. The average is shown for the longitudinal centreline. It is clear that the first portion of the test section has higher deflections (therefore lower stiffnesses) than the second part. This variation in deflections across the test sections explains the differences in the measurements obtained from MDDs on the same test section.

After water was added to the test sections, the deflections appeared to decrease, which was unexpected. The deflections were influenced by the extent of the cracking on the test section, and the amount of surface cracking increased dramatically after water was added.

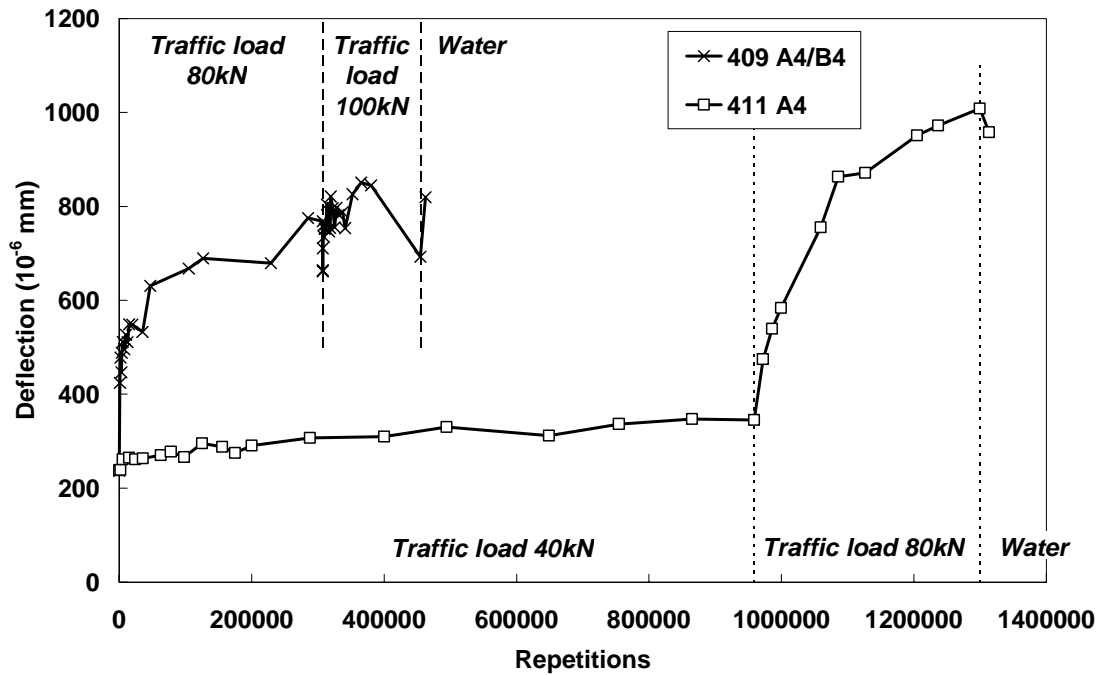


Figure 6. Elastic Surface Deflection Measured with the RSD

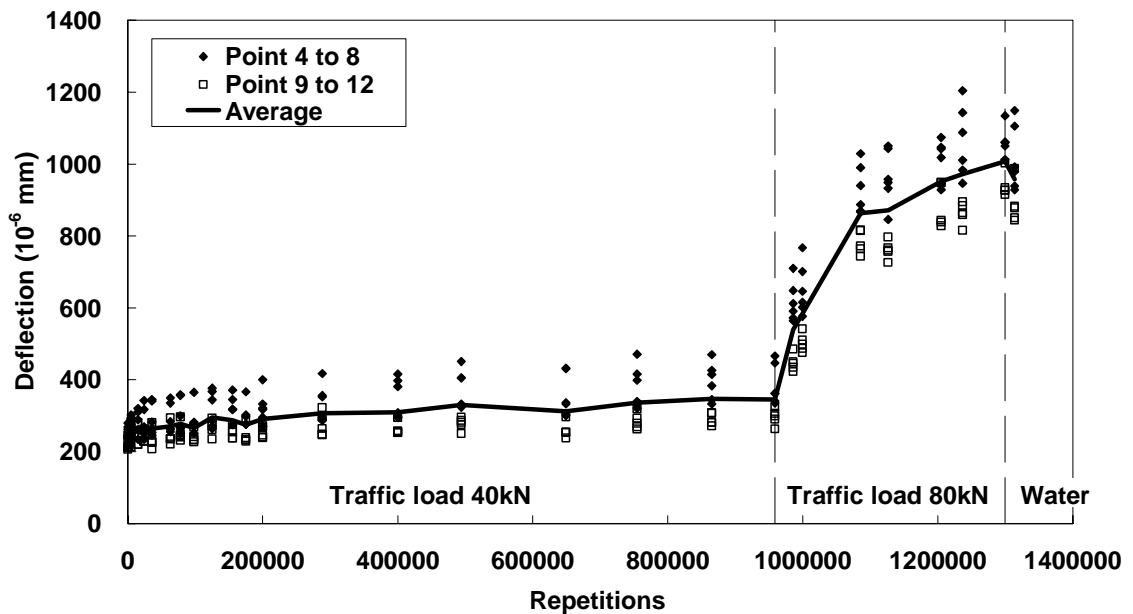


Figure 7. Elastic Surface Deflections Across Section 411A4

2.4.4 Back-calculated Elastic Stiffness

The elastic deflections measured in-depth with the MDDs were used to back-calculate the effective elastic stiffness values for the various pavement layers. Regardless of the

trafficking load, the stiffnesses are back-calculated from the deflection caused by a 40 kN dual wheel load. The HVS loads the pavement with dual wheels on a half axle. A 40 kN load is therefore assumed to transmit 20 kN through each tyre. This 40 kN HVS dual wheel load is equivalent to a standard axle load of 80 kN.

The stiffness values of the base layers are shown in Figure 8 for both test sections. The data for all the MDDs on each test section are shown to demonstrate the variability in stiffness experienced along the test sections. The scatter in the data is due to the scatter in the deflection data, which is, in turn, largely due to variability in the materials and construction. The back-calculation procedure is also sensitive to small changes in the measured deflections. Despite this variability, which is typical for pavements, trends are still clearly observable.

The initial stiffness of the materials is highly variable. For Section 409A4, the initial stiffness is between approximately 900 and 1100 MPa. Section 411A4 shows a large amount of variability, with an initial stiffness between 1250 and 3100 MPa. Because the initial stiffness is measured after 10 repetitions, the test sections trafficked with the higher starting load had a lower initial stiffness, which demonstrates the rapid reduction in stiffness in the early stages of a test. This rapid reduction in stiffness is similar to the behaviour of cement treated materials⁷.

As the test progressed, the elastic stiffness of the base layer reduced. This reduction was at a faster rate in the early stages of the test, and then decreased very gradually, seemingly to an asymptotic value. For Section 411A4 under the 40 kN load, the stiffness appeared to be decreasing gradually and had not reached a terminal value at the end of the test. When the load was increased to 80 kN, the stiffness decreased to approximately 250 to 550 MPa, with an average of approximately 400 MPa. The terminal value under the 80 kN load on Section 409A4 was approximately within the same range, and increasing the load to 100 kN did not result in a further decrease in the elastic stiffness. This indicates that, regardless of the load, the foamed bitumen treated material ultimately reaches the same equivalent granular state. From the trend in the data it seems reasonable to assume that, under the 40 kN load, the same equivalent granular state would have been reached. This material is very load sensitive in that the trafficking load determines the number of repetitions to reach the equivalent granular state.

The term “equivalent granular state” is used to describe the loss in resilient modulus (stiffness) of the material and is comparable to granular materials only in the stiffness and not in the physical composition of the materials. The term does not imply that the material is in a loose condition consisting of individual particles. The reduction in stiffness results in:

- less protection for the underlying layers;
- possibly higher shear stresses within the layer relative to the shear strength of the material, and
- increased horizontal strains at the bottom of the asphalt layer, contributing to increased asphalt fatigue.

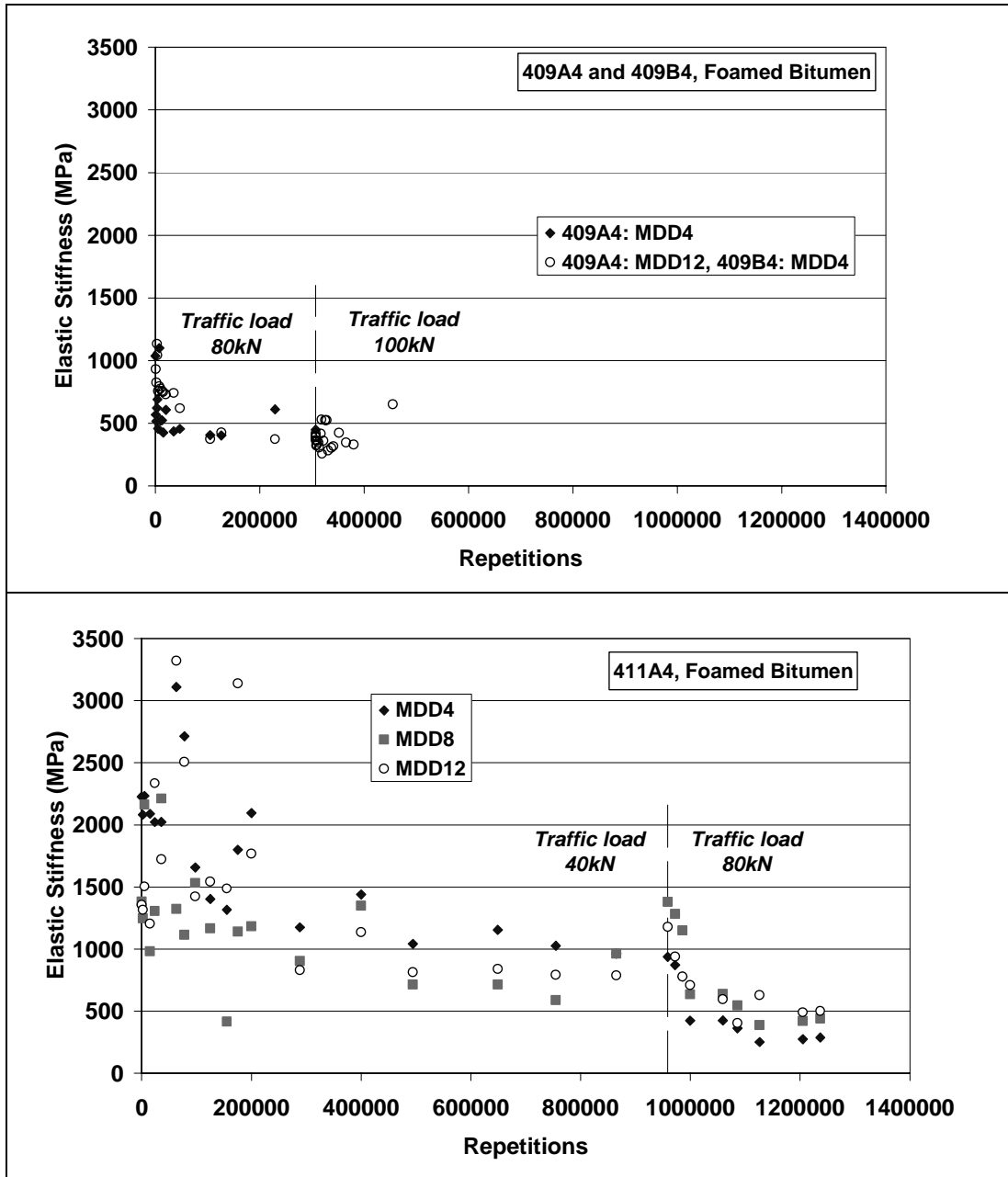


Figure 8. Back-calculated Base Layer Stiffnesses from MDD Measured Deflections

Elastic stiffnesses were not determined for measurements taken at different wheel loads at the same time. This would have allowed the stress dependency of the foamed bitumen material to be evaluated.

The HVS sections are treated with 2 percent cement and 1.8 percent foamed bitumen. At different combinations of cement and foamed bitumen, the behaviour may not be the same as experienced in the HVS test sections. However, without data for different combinations to suggest otherwise, it is reasonable to expect some similarities in the behaviour, in that a reduction in stiffness to an equivalent granular state under loading will be experienced. The time to reach an equivalent granular state is likely to be different for different combinations of cement and foamed bitumen. The HVS test sections were tested in a fairly short time period and therefore do not account for environmental influences, such as ageing. It is not thought that environmental influences would cause significantly different behaviour to that observed on the test sections, although the effects thereof should be evaluated with observations of field performance.

The elastic stiffness data were used to determine a structural design model for effective fatigue in Chapter 4.

2.5. Visual Observations

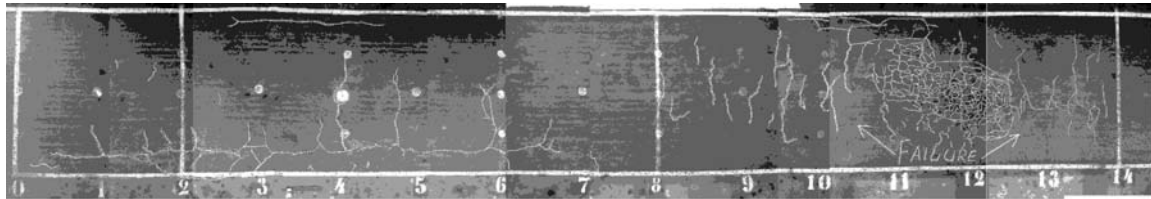
The surface cracking of the test sections was monitored visually and recorded on camera. The test sections showed very good performance, with very little visible surface cracking and rut depths of less than 7 mm before the addition of water. In general, when the sections are trafficked with the addition of water, the distress accumulated rapidly, with severe surface cracking being experienced. The tests were stopped when continuous trafficking on the disintegrating surface had the potential to damage the HVS. Photographs of the completed test sections are shown in Figure 9.

Section 409A4 had no surface cracking at the end of the 80 kN tests. The HVS was subsequently moved 4 metres along the test section and trafficking continued on Section 409B4. Half of Section 409B4 therefore continued trafficking Section 409A4 and the other half trafficked a previously unloaded part of the test section. A few cracks appeared on Section 409B4 before the addition of water. After the addition of water, it was noticed that the fines from the base had been pushed to the sides of the test section, causing small “humps” and the fines pumped through the cracks.

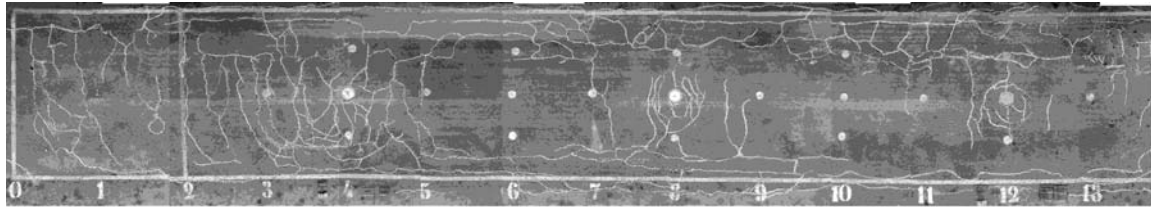
Section 411A4 also had very few cracks before the addition of water, but the addition of water resulted in MAD. Pumping was also experienced. A test pit across the test section

indicated the movement of fines from the trafficking area to the sides of the test section between the base layer and the asphalt surfacing. This showed that the loading reduced the bond between the surfacing and the base, generating fines. High tyre inflation and water pressures forced the fines to move away from the loaded area.

On all the test sections, the distress from surface cracking was more critical than that from permanent deformation.



Section 409B4



Section 411A4

Figure 9. Crack Patterns on HVS Test Sections

3. LABORATORY TESTING

A laboratory testing program was conducted in conjunction with the HVS testing. The materials were tested to determine the: tensile, compressive and shear strengths; flexibility; and permanent deformation resistance. These tests were part of a wider laboratory testing program involving untreated materials, and materials treated with cement, foamed bitumen and bituminous emulsion. Only the results of tests on the foamed bitumen treated materials are discussed in this report. All the laboratory tests and results are described by Long¹ and Robroch⁵.

The materials tested in the laboratory testing program were obtained from the HVS site after milling, and therefore includes some of the original surfacing (multiple seals) and ferricrete from the cement stabilised base and the untreated subbase. This material was treated with cement and foamed bitumen in the laboratory. The specimen preparation is described by Long¹ and Robroch⁵.

Several laboratory tests were run, including:

- indirect tensile strength test (ITS);
- unconfined compressive strength test (UCS);
- flexural beam test;
- static triaxial tests, and
- dynamic triaxial tests.

The ITS tests are not discussed in this report because the data were not directly used in developing the transfer functions.

3.1. Unconfined Compressive Strength (UCS)

The compressive strength of the foamed bitumen treated materials was determined using the unconfined compressive strength (UCS) test. The results are shown in Table 2. The results show that increased cement contents increase the compressive strength. However, increasing the foamed bitumen content with a constant cement content decreases the compressive strength. The UCS of the material treated with 2 percent cement only was approximately 3200 MPa, which is significantly higher than the UCS of the foamed bitumen treated materials. These results are discussed again in Section 3.6 and, in more detail by Long¹ and Robroch⁵.

Table 2. UCS Test Results

Sample	Binder Content %	Cement Content %	Density kg/m²	Moisture Content %	UCS kPa
FTB1	1.8	2	1978	11.4	1809
FTB2	1.8	2	1985	10.4	1864
FTB3	1.8	2	1961	10.9	1699
FTB7	3.0	2	1878	10.9	1124
FTB8	3.0	2	1886	10.3	1206
FTB9	3.0	2	1869	10.6	1096
FTB7	3.0	1	1953	10.6	877
FTB8	3.0	1	1952	10.6	822
FTB9	3.0	1	1957	10.6	905

3.2. Flexibility

The flexibility of the treated materials was determined with the flexural beam test. In this test, a constant, monotonic load is applied and the strain-at-break measured. This is equal to the strain at the point of crack initiation. The strain-at-break value provides an indication of the fatigue resistance of the material. Beams with a range of cement and foamed bitumen contents were tested. These results are shown in Figure 10 as a function of the foamed bitumen binder content.

Increasing the foamed bitumen content in the mix increases the flexibility of the material as indicated by the increase in the strain-at-break. The material is also more flexible at the lower cement contents. The tensile strength of the material, indicated by the stress-at-break, also increases with an increase in foamed bitumen content. By doubling the cement content from 1 to 2 percent, the stiffness of the mixes more than triples. The initial stiffness is approximately three times the stiffness-at-break.

For fatigue resistance, the optimal mix should contain some cement to provide tensile strength and a high foamed bitumen content to provide flexibility. The appropriate proportions of cement and foamed bitumen for a particular situation should be determined in the mix design. If the foamed bitumen content is too low, the mix has flexibility similar to that of a cement only treated material so that the use of low foamed bitumen contents is not justified¹.

Table 3. Flexural Beam Test Results

Sample	Foamed Bitumen Content (%)	Cement Content (%)	Stress-at-break (kPa)	Initial Stiffness (MPa)	Stiffness-at-break (MPa)	Strain-at-break (microstrain)	Strain-at-break Average and Standard Deviation
BM 2-5	1.8	1	76	820	303	251	240 11
BM 2-8	1.8	1	74	825	303	238	
BM 2-12	1.8	1	62	815	289	230	
BFTFB1	3.0	1	140	650	233	600	490 102
BFTFB2	3.0	1	133	660	239	557	
BFTFB4	3.0	1	116	605	220	527	
BFTFB5	3.0	1	111	765	280	396	
BFTFB6	3.0	1	126	946	341	369	
BM 3-10	5.0	1	177	407	143	848	837 68
BM 3-13	5.0	1	107	396	140	764	
BM 3-14	5.0	1	193	595	215	898	
FTB 1	1.8	2	230	5975	2085	111	172 52
FTB 3	1.8	2	20	352	123	162	
FTB 2	1.8	2	307	3843	1301	236	
FTB 5	1.8	2	294	4950	1644	179	
FTB 7	3.0	2	382	3420	1139	335	352 52
FTB 8	3.0	2	270	2483	784	344	
FTB 9	3.0	2	192	1350	451	426	
FTB 10	3.0	2	310	3019	1037	299	
FTB 11	3.0	2	342	3229	1115	307	
FTB 12	3.0	2	325	2288	804	404	

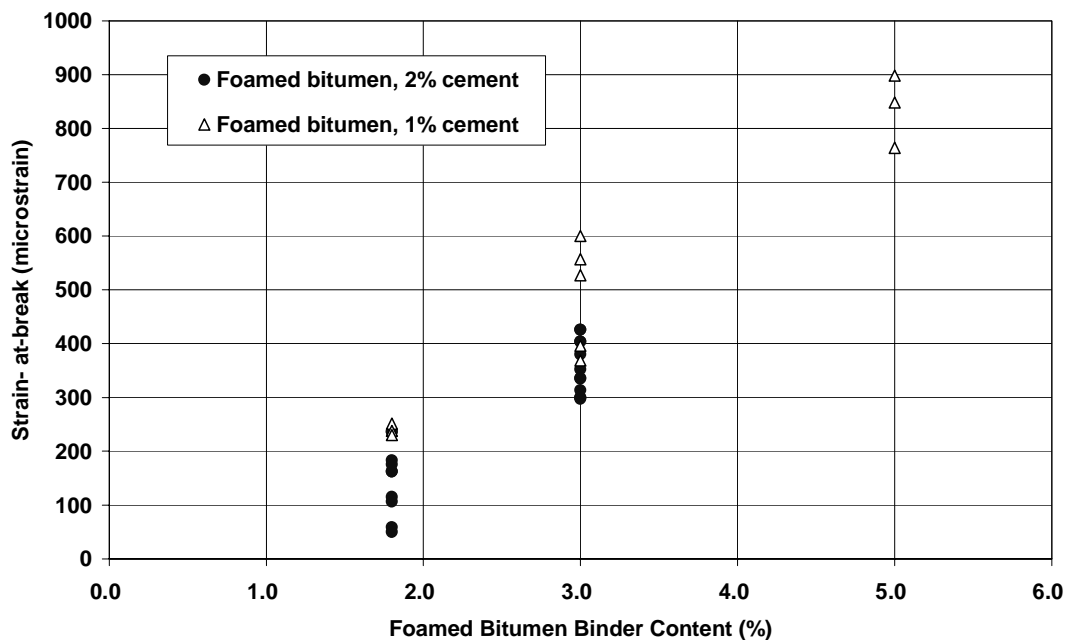


Figure 10. Strain-at-break

3.3. Shear Strength

The shear strength, in terms of the friction angle and cohesion, is determined using the static triaxial test^{1, 6}. The tests were run at two densities and two saturation levels for the foamed bitumen treated materials with 2.0 percent cement and 1.8 percent residual binder, and 1.0 percent cement with 3.0 percent residual binder. Relative density (RD) and saturation (S) are calculated using Equations (1) and (2), respectively. The term “relative density” used in this report refers to the ratio of the dry density to the AD, as shown in Equation (1). The apparent relative density is the density of the material relative to the density of water.

$$RD = \frac{\text{dry density}}{AD} \tag{1}$$

$$S = \frac{\frac{MC}{100} \cdot \frac{\text{dry density}}{1000}}{1 - RD} \tag{2}$$

- where RD = relative density
- AD = apparent density = ARD • density of water
- ARD = apparent relative density (specific gravity)
- S = saturation
- MC = moisture content

The high and low relative density values are approximately 73 and 70 percent, respectively. The high and low saturation levels are between approximately 56 to 59 percent and 33 to 44 percent, respectively.

The static triaxial tests were run at four confining pressures (20, 80, 140 and 200 kPa) at each density and saturation level. This gave 16 tests per material type.

The results of the static triaxial tests are shown in Figure 11 for the four combinations of density and saturation. Increasing the residual binder and decreasing the cement contents of the foamed bitumen treated material reduces the cohesion and, in general, decreases the friction angle. The results are shown at low and high values of relative density and saturation. The actual density and saturation values are not necessarily the same for all the materials, which accounts for some of the variability and inconsistencies in the data. The low saturation mixes with 1 percent cement and 3 percent foamed bitumen were at an average of 33 percent saturation, which is a moisture content of 5 to 6 percent. This saturation is very low, which accounts for the relatively high friction angle and cohesion values obtained for this combination.

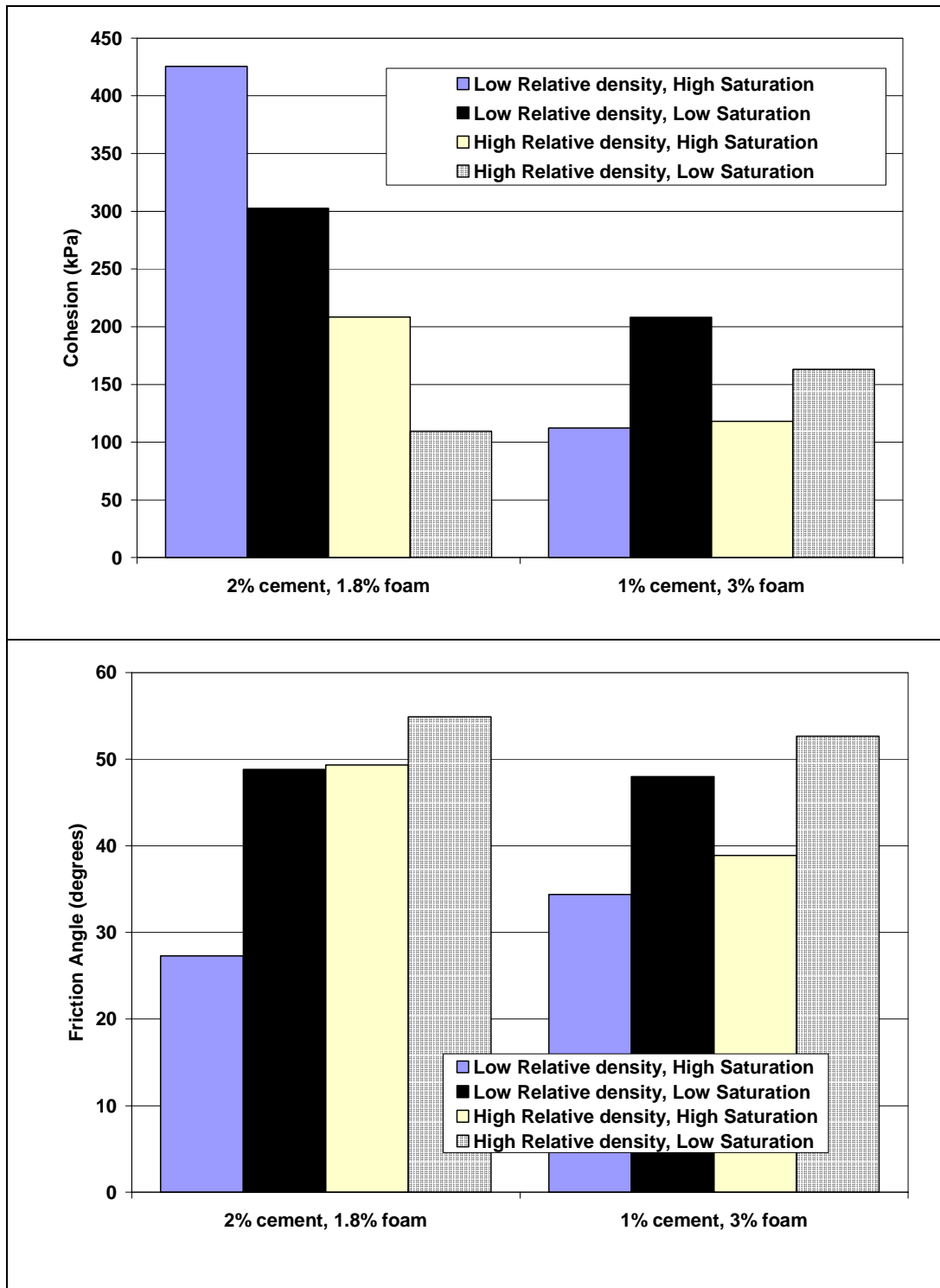


Figure 11. Cohesion and Friction Angle from Static Triaxial Test

3.4. Elastic Stiffness (Resilient Modulus)

The dynamic triaxial test is used to determine both the resilient modulus (stiffness) and the permanent deformation response of the materials. The measured stiffness is a compressive modulus. The dynamic triaxial tests were performed at two densities and saturation levels. The tests were run at two confining stresses (80 and 140 kPa) and three stress ratios (0.20, 0.55 and 0.90). A total of 24 dynamic triaxial tests were run per material combination. The stress ratio is calculated using Equation (3). The vertical stress or major principal stress for the triaxial test was calculated for the required stress ratio. Alternatively, knowing the applied major and minor principal stresses, and the cohesion and friction angles for the material, the stress ratio is calculated using Equation (3).

$$SR = \frac{\sigma_1^a - \sigma_3^a}{\sigma_1^m - \sigma_3^a} = \frac{\sigma_1^a - \sigma_3^a}{\sigma_3^a \left(\tan^2 \left(45^\circ + \frac{\phi}{2} \right) - 1 \right) + 2C \tan \left(45^\circ + \frac{\phi}{2} \right)} \quad (3)$$

- where σ_1^a = applied major principal stress
 σ_1^m = maximum allowable major principal stress
 σ_3^a = applied minor principal stress
 C = cohesion
 ϕ = friction angle

The resilient modulus was measured on each specimen. Regression models were fitted to the data as a function of the relative density, saturation, confining stress and stress ratio. The regression models for the treated materials did not show a good correlation and were relatively insensitive to the input variables¹. This is partly due to the variability in the test data but also indicates that, by treating the materials, the sensitivity to the relative density and saturation is reduced. Because of the insensitivity of the resilient modulus to relative density, saturation and stress ratio, it is recommended that the average stiffness of the treated materials, shown in Table 4, be used for design purposes.

Table 4. Ranges of Resilient Modulus Values

	2% Cement 1.8% Foamed Bitumen	1% Cement 3.0% Foamed Bitumen
Minimum	1200	450
Maximum	2600	2000
Average	1657	1154
Standard Deviation	419	470
Coefficient of Variation	0.25	0.41

The stiffness is lower at the lower cement and higher foamed bitumen contents, showing the additional stiffness that the additional cement provides. These stiffness values differ from the stiffness values shown in Table 3 for the flexural beam. This is because the stiffness measured in the dynamic triaxial test is a compressive stiffness whereas the flexural beam test measures a tensile stiffness. The compressive stiffness is greater than the tensile stiffness, which is typical for pavement materials. The difference in stiffnesses between the two combinations of cement and foamed bitumen is greater for the tensile stiffness than the compressive stiffness. This indicates that increasing the foamed bitumen content and decreasing the cement content has a greater influence on the flexural properties than on the compressive properties of the mix.

The resilient modulus values from the dynamic triaxial test are in the same range as the initial resilient modulus values back-calculated for the base layer of the HVS test sections (see Figure 8). This gives confidence to the values obtained from the dynamic triaxial test and seems to indicate that the laboratory test values provide representative pavement stiffness values, which can be used in pavement design. This should be confirmed with more comparisons of laboratory and back-calculated values.

3.5. Permanent Deformation

Dynamic triaxial tests were performed to assess the permanent deformation behaviour and structural capacity of the mix. The term “structural capacity” is the same as the term “bearing capacity” used in the South African Mechanistic-Empirical Design Method and, in this report, refers to the permanent deformation structural capacity. The variables tested were described in Section 3.4. A model, of the form shown in Equation (4), was fitted to all the reasonable data for each specimen. For the data fitted, the model fits were reasonable¹.

$$PD = mN + \frac{cN}{\left[1 + \left(\frac{cN}{a}\right)^b\right]^{\frac{1}{b}}} \quad (4)$$

where PD = permanent deformation (mm)
m, a, b, c = regression coefficients
N = load repetitions

The regression models were used to calculate the structural capacity (load repetitions) to a specific plastic strain (PS). These values were used with the relative density (RD), defined in Equation (1) and Section 3.3, and stress ratio (SR) to develop a regression model predicting the structural capacity for each material. The form of which is shown in Equation (5). Also included in the model is a term for the ratio of the cement to foamed

bitumen contents (cem/bit). The letters a to e are regression coefficients. The R^2 and standard error of the estimate for this model are 0.81 and 0.29, respectively. The stress ratio (SR) is defined in Equation (3).

$$\log N = a + b \cdot RD + c \cdot PS + d \cdot SR + e \cdot (\text{cem/bit}) \quad (5)$$

The differences between the permanent deformation behaviour of the two mixes are not adequately accounted for in the stress ratio and relative density terms above. To be able to have one model that is useful to foamed bitumen mixes with various cement and foamed bitumen contents it is necessary to include a term such as the cement to foamed bitumen content ratio, as shown in Equation (5) to account for the different behaviour of the mixes at the different cement and binder combinations. With the limited data available, the ratio used seems a logical choice because it can account for variations in both cement and foamed bitumen contents and the interaction between the two. Whether this linear ratio is the best term to use can only be evaluated with additional data.

The structural capacity to 5 percent plastic strain of the foamed bitumen materials assuming a relative density of 0.7 is shown in Figure 12 as a function of the stress ratio. A relative density value of 0.7 is similar to the relative density of the HVS test section. The increase in the foamed bitumen binder content and associated decrease in the cement content reduces the permanent deformation resistance of the materials.

The model shown in Equation (5) is discussed in more detail in Chapter 4 and will be combined with the HVS permanent deformation results to develop a field calibrated permanent deformation design model.

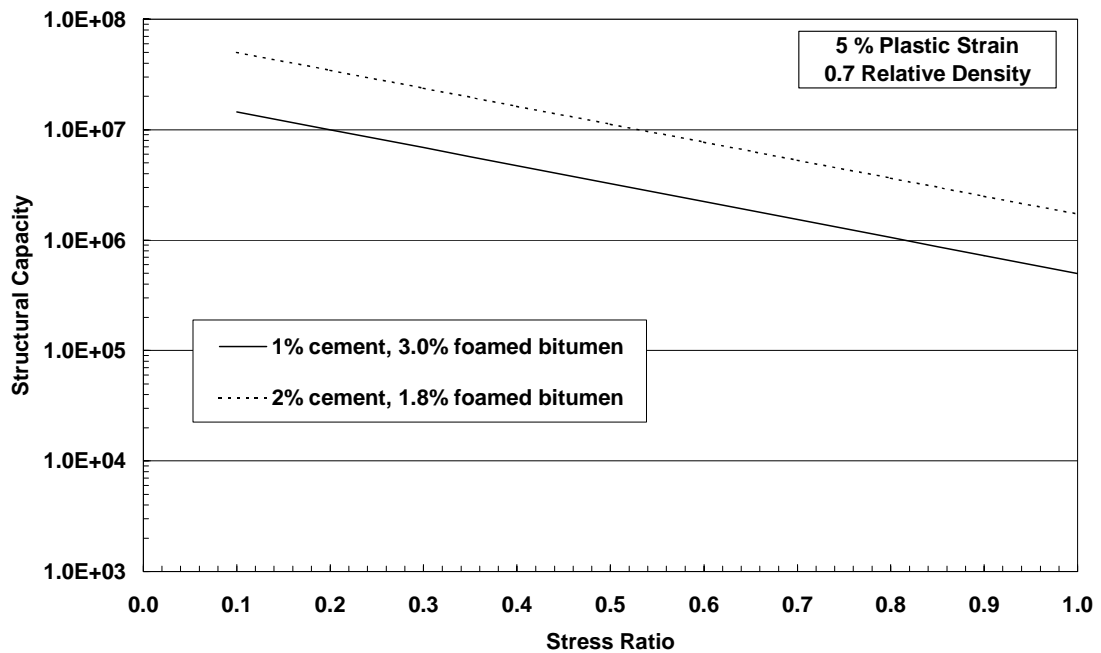
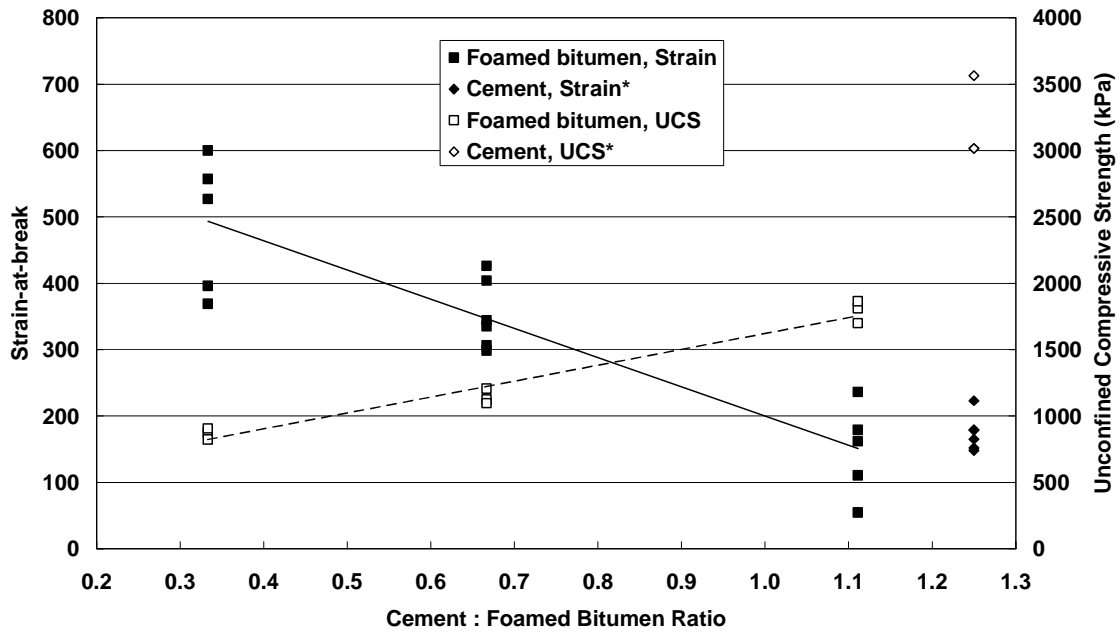


Figure 12. Structural Capacity Model from Laboratory Permanent Deformation Tests

3.6. Discussion

The laboratory testing results show that, by treating the materials with foamed bitumen and cement, their properties are improved. The addition of cement significantly contributes to the permanent deformation resistance, and the addition of foamed bitumen significantly contributes to the flexibility of the material. This is demonstrated in Figure 13 where the strain-at-break values from the flexural beam tests are plotted on the left hand side vertical axis, as a function of the ratio of the cement to foamed bitumen contents. The strain-at-break values give an indication of the flexibility and, therefore, the fatigue resistance of the materials. The unconfined compressive strength (UCS) values are plotted on the right hand side vertical axis, also as a function of the ratio of the cement to foamed bitumen contents. The UCS values give an indication of the compressive strength, and therefore the permanent deformation resistance of the materials. A linear trend line is shown for each set of values. The crossover point of the two trend lines has no significance as it depends on the scales used on both vertical axes. It should therefore not be used to select optimum cement and foamed bitumen contents. Also included in the chart are the data for the same milled material treated with 2 percent cement and no foamed bitumen, plotted at an arbitrary ratio of 1.25. The ratio for cement only is actually infinity, and therefore plots off the scale shown. The cement treated material is discussed by Long¹.



* Cement treated with 2 percent cement and no foamed bitumen. Values plotted at an arbitrary ratio of 1.25.

Figure 13. Strength and Flexibility of Foamed Bitumen Treated Materials

Figure 13 clearly shows how the flexibility of the material decreases with an increase in the cement to foamed bitumen content ratio, whereas the compressive strength increases. The addition of foamed bitumen contributes significantly to the fatigue resistance of the mix, although, if not enough foamed bitumen is added, these benefits are significantly reduced. Some minimum compressive and flexural strength is needed in the material and this is best provided by the addition of cement. The exact proportions of cement and foamed bitumen that should be included in a mix depend on the specific project, and the balance of flexibility to compressive and flexural strengths required.

Effective fatigue of the HVS test sections was the more dominant distress. Although the surface cracking was not extensive, there was relatively more fatigue damage than the little permanent deformation experienced. By increasing the bituminous binder content and possibly reducing the cement content the material would have had greater fatigue resistance, which could be expected to provide a longer pavement life before surface cracking, without having resulted in excessive permanent deformation.

4. STRUCTURAL DESIGN AND PERFORMANCE MODELS

From the HVS and laboratory test data, it is possible to develop structural design and performance models for use in mechanistic-empirical pavement design. This chapter discusses the development of such models for foamed bitumen treated pavement layers.

4.1. Design Philosophy

The philosophy used to develop the structural design procedure is founded on examining the material behaviour and distress mechanisms in the pavement from the HVS tests, and in the laboratory. This behaviour is then related to engineering parameters determined from mechanistic analyses of the pavement structure. Transfer functions are developed relating the observed distress to the engineering parameters.

The process involves interpolating and extrapolating the available data to obtain a general procedure applicable to a wider range of pavement types and foamed bitumen layers. The interpolating, extrapolating and the development of the transfer functions rely heavily on engineering judgement. This is the same philosophy used to develop the South African Mechanistic-Empirical Design Method⁷ and TRH4⁸.

The two major forms of distress on the HVS test sections are permanent deformation and effective fatigue. Structural design and performance models are determined for both modes of distress.

4.2. Permanent Deformation

The structural design model for permanent deformation of the foamed bitumen treated material is developed from the in-depth permanent deformation of the base layer measured by the MDD and the permanent deformation response measured in the laboratory with the dynamic triaxial test. The model predicts the permanent deformation of the base layer only. In the mechanistic-empirical design procedure the permanent deformation of the other layers is determined using the models applicable to the material type used for the layer.

4.2.1 Regression Model for In-depth MDD Permanent Deformation Data

The first step in developing a structural design model is to fit a regression model of the form shown in Equation (6) to the MDD permanent deformation data for the base layer.

an example of which is shown in Figure 5. Justification for the selection of this model is discussed by Theyse⁶.

$$PD = mN + a(1 - e^{-bN}) \quad (6)$$

were PD = permanent deformation in the base layer (mm)
 m, a, b = regression coefficients
 N = load repetitions

Because of the variation in MDD data along a test section, the model is fitted to each MDD from both test sections, rather than averaging the data. To determine the permanent deformation for the treated base layer only, the deformation of the MDD module at 275 mm is subtracted from the deformation of the top MDD module (25 mm). The model fits and the data are shown in Figure 14. All the model fits are reasonable. Only the data from the first loading sequence for each test section were used in these analyses. The data for the higher wheel load used in the second sequence have a load history which is difficult to account for and are therefore excluded from the analyses.

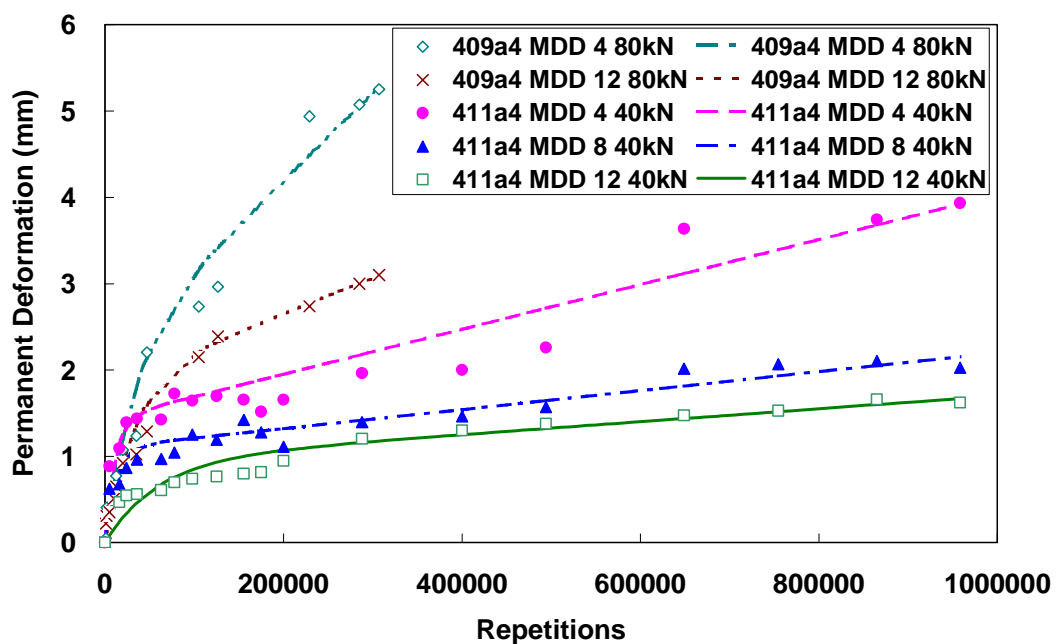


Figure 14. Base Layer MDD Permanent Deformation Regression Model Fits

4.2.2 Permanent Deformation Model from HVS Data

Using the regression model from the MDD data it is possible to determine a simple equation to predict the repetitions to a certain level of permanent deformation (or plastic strain) for a given wheel load. The model is formulated in terms of plastic strain to allow

for the use of different layer thicknesses. The plastic strain is the ratio of the permanent deformation to the initial layer thickness, as a percentage.

The model is calibrated by determining the permanent deformation (or plastic strain) for a series of repetitions generated using Equation (6). This gives a range of data for each wheel load and MDD. These data, for all the MDDs, are then used to fit a model, shown in Equation (7).

$$\log N_{PD,FB} = a + b \cdot PS + c \cdot WL \quad (7)$$

where $N_{PD,FB}$ = permanent deformation load repetitions, foamed bitumen treated material

PS = plastic strain (%)

WL = wheel load (kN)

a, b, c = regression coefficients

Some of the data used to fit the model, and the model itself are shown in Figure 15 as a function of the HVS dual wheel load. It is important to note that this model is only applicable to the specific pavement structure and material properties at the HVS test site.

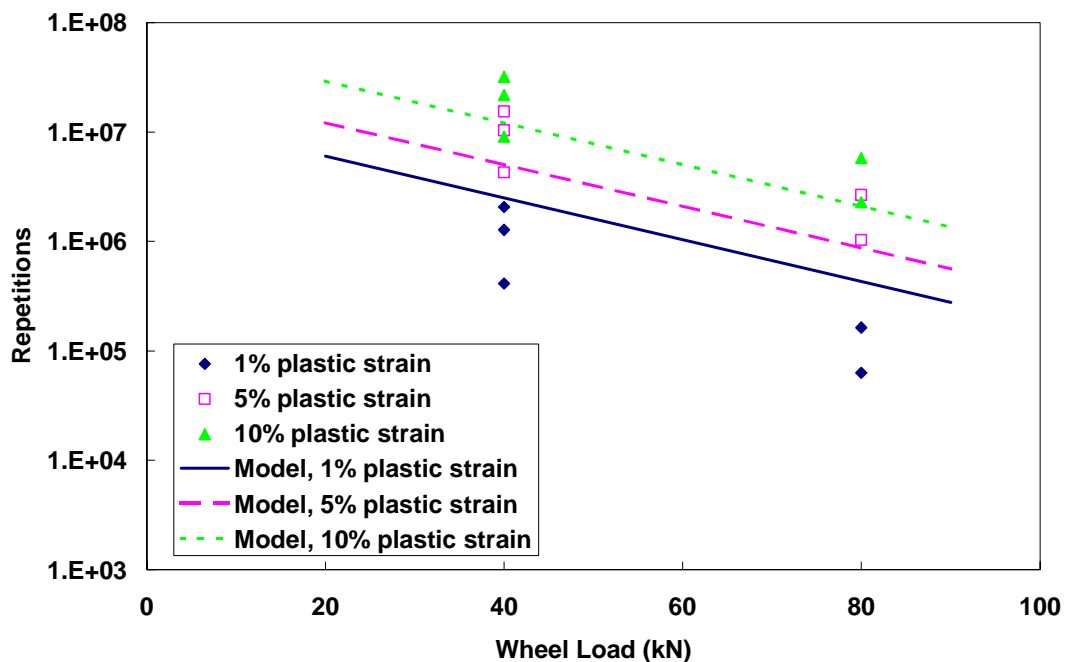


Figure 15. HVS Derived Permanent Deformation Model for Foamed Bitumen Treated Material

The HVS derived structural capacity model, Equation (7), is equivalent to the laboratory derived model, Equation (5), and both can be used to make an estimate of the structural capacity or load repetitions to a certain level of permanent deformation. The HVS derived

model is, however, limited in its application as it is specific to the pavement structure and conditions on the HVS site and is a function of wheel load and not applied stress. The laboratory derived model incorporates a much wider set of conditions than the HVS model, but is not calibrated for field conditions. By combining the desired characteristics of the two models into one calibrated model, a final design model is obtained that may be used with some confidence. This process is applied to the laboratory and HVS derived models for the permanent deformation of the foamed bitumen treated material in the following sections.

4.2.3 Mechanistic Pavement Analyses for Permanent Deformation

For general design and analyses purposes it is necessary to have a transfer function that estimates the structural capacity of any pavement structure with a foamed bitumen treated layer. This should account for the different material properties of the treated layer from pavement to pavement. This is typically done by estimating material properties from laboratory or field testing, or from recommended values, and then analysing the pavement to determine a mechanistic parameter that is related to the structural capacity.

In the South African Mechanistic-Empirical Design Method (SAMDM) and TRH4, the pavement structures are usually modelled using multi-layer linear elastic theory^{7,8}. This theory has several drawbacks, and cannot directly predict the permanent deformation response of the pavement nor account for any non-linear behaviour. However, more appropriate advanced models have not been calibrated for pavement materials and will not be widely used in industry for many years. The SAMDM currently assumes all materials are linear elastic. Linear elasticity is therefore used in the structural design procedure for foamed bitumen treated materials.

A mechanistic parameter which has been recommended for granular materials is the stress ratio, defined in Equation (3)⁶. In an analysis of a pavement structure, the stress ratio is calculated using the major and minor principal stresses, and the cohesion and friction angle of the material. The stress ratio is the inverse of the factor of safety, which is the mechanistic parameter currently recommended in the SAMDM. Theoretically, a stress ratio greater than one indicates a shear stress failure. It was decided to develop the permanent deformation transfer function as a function of the stress ratio. This entails determining the critical (maximum) stress ratio in the foamed bitumen treated layer and using this parameter in the place of the wheel load in Equation (7) and Figure 15.

Stress Ratio Calculation

One of the problems with linear elasticity is that tension is allowed in the material. This is not representative of the behaviour of granular materials, which typically cannot exhibit tension. For the type of mechanistic analyses typically performed on pavement layers, this problem manifests itself as unreasonably low or even tensile values for the minor principal stress. In the SAMDM it is recommended that this problem be dealt with by setting the unreasonable tensile minor principal stress values equal to zero, and by adding the magnitude of the minor principal stress to the major principal stress so that the deviator stress is unchanged⁷. This results in more reasonable values.

A common geotechnical method of calculating the horizontal stress (σ_h) as a function of the vertical stress (σ_v) is shown in Equation (8) where k_0 is calculated using Equation (9) from the friction angle, ϕ . To use this method, the vertical stress is calculated from a multi-layer linear elastic analysis. To calculate the stress ratio, it is assumed that the horizontal and vertical stresses are approximately equal to the minor and major principal stresses. In the areas of interest in the pavement this assumption is acceptable.

$$\sigma_h = k_0 \cdot \sigma_v \quad (8)$$

$$k_0 = 1 - \sin \phi \quad (9)$$

The stress ratio was calculated from the major and minor principal stresses from a linear elastic analysis, and from the major principal stress and Equations (8) and (9). The weight of the overburden was not included in the calculation of the horizontal stress in the k_0 method. The stress ratio from the k_0 equations decreases with depth, because the vertical stress decreases with depth. Using the k_0 method of calculating the stress ratio, it was also found that the difference between the stress ratios for 40 kN and 80 kN wheel loads was not significant. This is not reasonable as pavements experience more damage under a heavier wheel load than under a lighter wheel load. The small difference in the stress ratios for the different wheel loads calculated using k_0 does not adequately reflect the difference in damage.

The stress ratios calculated from the major and minor principal stresses were more reasonable and differentiate between wheel loads, despite the problems with linear elasticity. It was therefore decided to use the stress ratio calculated from the major and minor principal stresses in a multi-layer linear elastic analyses. The values are adjusted, as described above, if the minor principal stress is tensile.

Location of Critical Stress Ratio

Traditionally in TRH4, granular materials are evaluated in the middle of the layer, between the tyres. To see if this is applicable to foamed bitumen treated materials, a pavement structure similar to the HVS test sections was analysed at two wheel loads to determine the location of the maximum stress ratio. An example of this analysis is shown in Figure 16 and Figure 18, for 40 kN, 620 kPa dual wheel loads. Figure 16 shows the maximum stress ratio with depth and Figure 18 shows the x and y coordinates of the location at which the maximum stress ratio is found. The wheel loads are applied at (x=0, y=-175) and (x=0, y=175), as shown in Figure 17. In this analysis, the foamed bitumen base layer was 245 mm thick, underneath a 30 mm surfacing. The depth of the foamed bitumen layer is therefore from 30 mm to 275 mm, which is shown in Figure 16. The maximum stress ratio at each depth was calculated. The results were similar for an analysis with 80 kN, 800 kPa dual wheel loads.

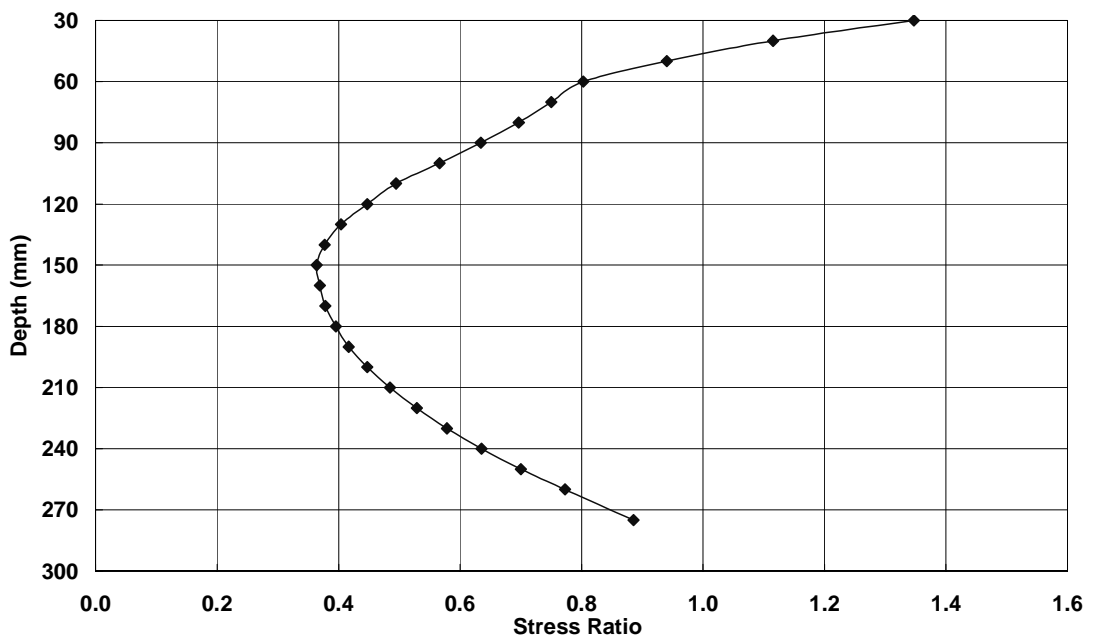


Figure 16. Maximum Stress Ratio

In Figure 16 it is clear that in the middle of the layer, the stress ratio has the smallest value and this is therefore not the critical location. The stress ratio is largest at the top and bottom of the layer. At the top of the layer, the stress ratio is a maximum under the tyres. However, as the depth increases the location rapidly moves to between the tyres and then back to a position underneath the tyre in the bottom half of the layer. The stress ratio values at the top and bottom of the layer are extreme values, as indicated by their magnitude being over 1. These values are not reasonable for routine analyses.

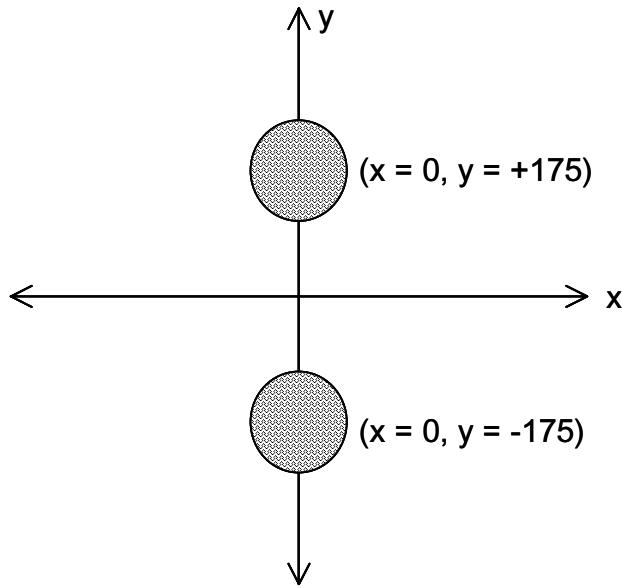


Figure 17. Location of Tyres in Analyses

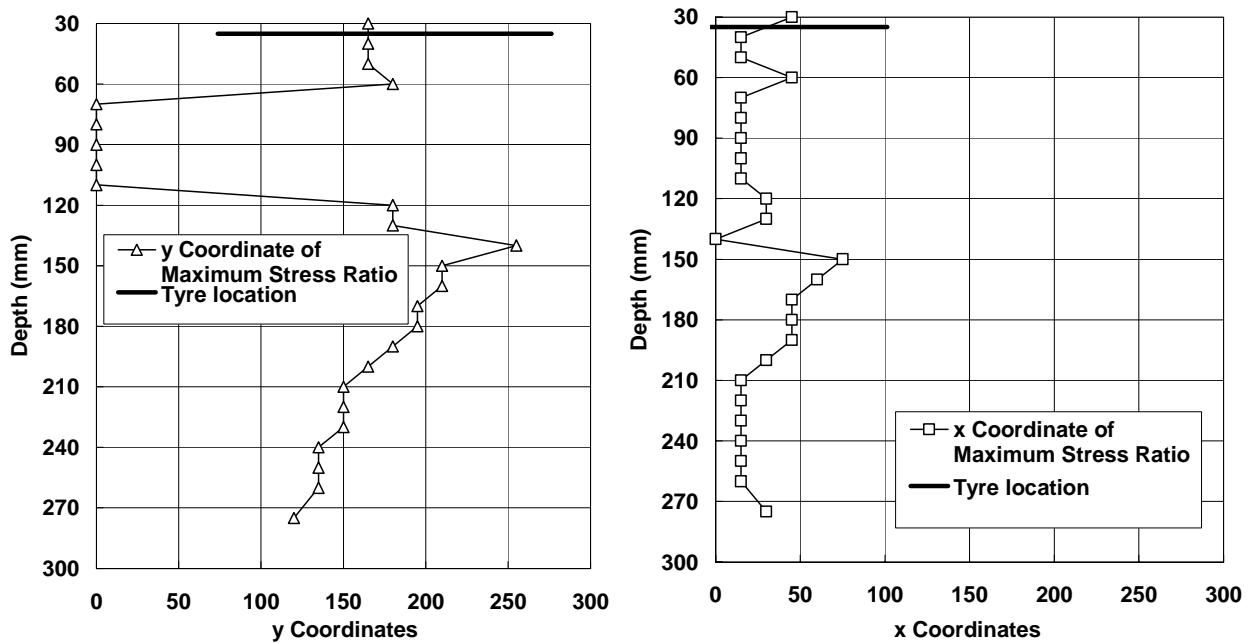


Figure 18. Location of Maximum Stress Ratio

It is not practical to specify in the design procedure that the stress ratio should be evaluated at all possible locations in the pavement. Specific locations should rather be recommended. For this reason, and from the analyses described above, it is recommended that the stress ratio be calculated at two depths in the pavement. The first depth is at one-quarter of the thickness of the layer. This represents the behaviour in the upper section of the layer. The second location is at three-quarters of the thickness of

the layer, which represents the behaviour at the lower section of the pavement. From the analyses described above, it appears as if the critical location in the upper portion of the pavement is in the area between the wheels and in the lower portion of the layer in the area underneath the wheel. However, from pavement analyses exactly under and between the wheels, both depths have the potential to be critical. At this stage, it is therefore recommended that the stress ratio is evaluated at all four locations, as shown in Figure 19. The largest of the four values should be used in the further analyses. With further pavement analyses, it is possible that a lesser number of locations would suffice.

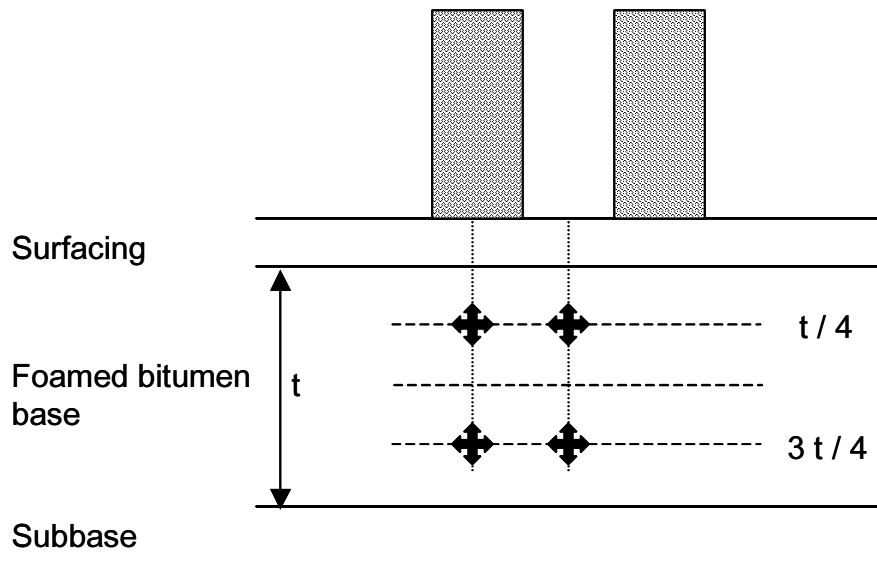


Figure 19. Recommended Locations to Calculate the Stress Ratio

HVS Test Section Stress Ratios

To determine the stress ratios of the HVS test sections, multi-layer linear elastic analyses were performed. The back-calculated MDD stiffnesses were used for the pavement layers, and the thicknesses were determined from the test pit data^{3,4}. Analyses were performed for all the MDDs on each test section.

The increase in permanent deformation in the HVS test sections is at a much more gradual rate than the reduction in stiffness. Much of the permanent deformation occurs once the foamed bitumen layer has reached the equivalent granular state. For this reason, if the initial stiffnesses of all the pavement layers are used in the analyses a very conservative stress ratio would be calculated for the foamed bitumen layer. The stress ratios were, therefore, determined using the back-calculated stiffnesses at the approximate point at which the equivalent granular state was reached in the foamed bitumen layer. A second method was also used in which stress ratios were determined using the initial stiffnesses for all layers other than the foamed bitumen treated layer, for

which the equivalent granular state value of 400 MPa was used. This second method is easier for routine design and follows the recommended SAMDM procedure for analysing the life of the different phases of the pavement. It was found that the stress ratio was not significantly different using the two sets of stiffness values. For ease of analysis, it is therefore recommended that the stress ratio be calculated using the initial stiffness of all layers except the foamed bitumen treated layer, for which the stiffness of the equivalent granular state should be used.

The equivalent granular state stiffness value of 400 MPa is valid for the HVS test sections and the material in the foamed bitumen base layer. This value may change for a different pavement structure or with a foamed bitumen material with a different combination of cement and foamed bitumen. However, it is expected that another material would still reach an equivalent granular state. Further research could identify whether the observed HVS behaviour is applicable to all types of foamed bitumen materials, and may also refine the expected value for the stiffness of the equivalent granular state.

The stress ratios calculated for the two or three MDDs within each test section showed little variation. For the 40 kN section, 411A4, the average stress ratio was 0.21 and for the 80 kN section, 409A4, the average stress ratio was 0.33. These values clearly differentiate between the wheel loads.

4.3. Development of Transfer Functions for Permanent Deformation

In the previous section, a transfer function was developed from the HVS data and the stress ratios calculated for the HVS test sections. This model is now used to calibrate the laboratory model, which can account for a wider range of material properties, to obtain a final recommended transfer function.

4.3.1 Transfer Function from HVS Data

A revised version of Equation (7) was fit using the calculated stress ratios for each MDD on both test sections, and the pavement life (structural capacity) to various levels of plastic strain. This function has the form shown in Equation (10), where the stress ratio (SR) replaces the wheel load in Equation (7). The data and the model fit are shown in Figure 20. The R^2 value for the fit shown in the figure is 0.76 and the standard error of the estimate is 0.35.

$$\log N = a + b \cdot PS + c \cdot SR \quad (10)$$

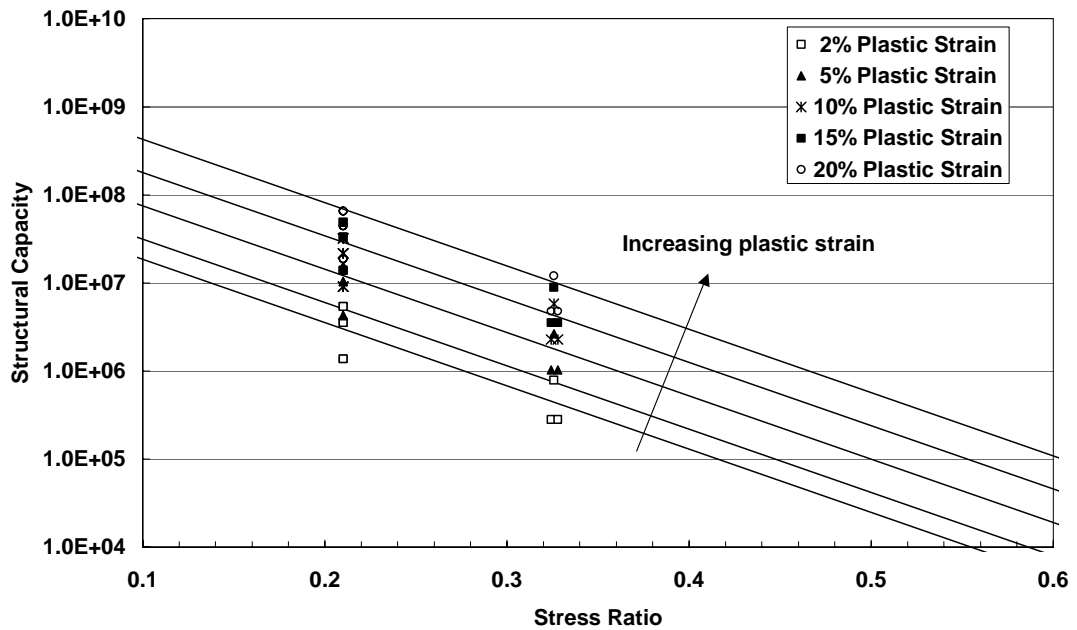


Figure 20. Structural Capacity as a Function of Stress Ratio from HVS Data

4.3.2 Permanent Deformation Transfer Function

The permanent deformation model from the dynamic triaxial tests (Equation (5)) is a function of the plastic strain, stress ratio, relative density and the cement to bitumen content ratio. The HVS transfer function shown in Figure 20 (Equation (10)) is for the specific combination of 1.8 percent foamed bitumen and 2 percent cement of the foamed bitumen layer in the HVS test sections. The HVS model also does not directly account for the relative density, although the relative density has an influence on the cohesion and friction angle values in the calculation of the stress ratio, so it is indirectly accounted for. To determine a transfer function that directly accounts for the relative density and is applicable to other cement and foamed bitumen contents, the laboratory model (Equation (5), Section 3.5) was calibrated with the HVS model. Using both models the structural capacities were calculated using: a range of plastic strains; the stress ratios calculated for the HVS pavements; and a relative density of 0.73, which is the estimated relative density of the HVS test sections. These results are shown as the solid diamonds in Figure 21, in which the results from the laboratory and HVS models are compared.

The laboratory model predicts a larger structural capacity than the HVS model, but the trends in the data are the same. The laboratory test was performed on new material that had not experienced damage. The loads were relatively small so the specimen was not significantly damaged during the test. Therefore, it is reasonable to expect that the structural capacity estimated using the laboratory model would be greater than for the HVS model. The boundary conditions of the HVS test are similar to those of a pavement

in the field, and it is therefore likely that the HVS results are closer to field results than the laboratory results. It is therefore reasonable to shift the laboratory model predictions to be in closer agreement with the HVS model predictions.

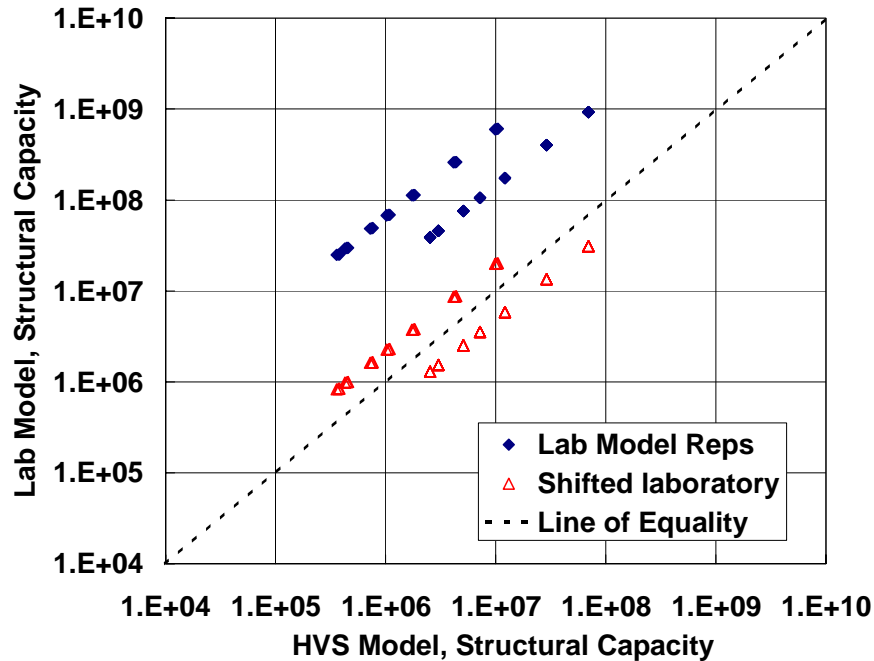


Figure 21. Comparison of Laboratory and Permanent Deformation HVS Transfer Functions

From Figure 21 it is clear that a linear shift in the laboratory estimated structural capacity would result in a much closer agreement with the HVS estimated values. A shift factor is calculated from the average of the ratio of the HVS and laboratory structural capacities for each data point. Dividing the laboratory value by a shift factor of 30 results in the open triangles shown in Figure 21. By incorporating this shift factor in the laboratory transfer function, the predicted values are in closer agreement with the HVS values. The actual magnitude of the shift factor will need to be checked and recalibrated with additional field data, especially for foamed bitumen materials with different combinations of cement and binder contents. Without HVS data at different combinations of cement and binder, it is not possible to determine a shift factor for other combinations. However, by calibrating the laboratory model with the HVS model at one specific combination of cement and binder, the confidence in the laboratory model is increased, especially within the range of stress ratios found in the pavement structures. Calibrations updated with additional data, as they become available, will further increase the confidence. The effect of the environment was not considered in the shift factor.

By calibrating the laboratory and HVS permanent deformation transfer functions as described above, a general transfer function to determine the structural capacity of all types of pavement structures with a foamed bitumen treated layer is developed.

Using the combined model, and examining the residuals between the actual and predicted values, it is possible to calibrate the model for different levels of reliability. The transfer functions for the different reliability levels, which correspond to the reliability associated with Category A to D roads, are shown in Equation (11) and in Figure 22 for an assumed plastic strain of 9 percent. According to the SAMDM, a reliability of 95 percent corresponds to Category A roads, 90 percent to Category B, 80 percent to Category C and 50 percent to Category D roads⁷. The R² of the original laboratory model from which Equation (11) was calibrated was 0.81, and only the statistically significant variables were included in the model.

Permanent Deformation Transfer Function:

$$\begin{aligned}
 \text{Category A: } N_{PD,FB} &= \frac{1}{30} \cdot 10^{[-2.047+11.938 \cdot RD+0.0726 \cdot PS-1.628 \cdot SR+0.691(\text{cem/bit})]} \\
 \text{Category B: } N_{PD,FB} &= \frac{1}{30} \cdot 10^{[-1.951+11.938 \cdot RD+0.0726 \cdot PS-1.628 \cdot SR+0.691(\text{cem/bit})]} \\
 \text{Category C: } N_{PD,FB} &= \frac{1}{30} \cdot 10^{[-1.816+11.938 \cdot RD+0.0726 \cdot PS-1.628 \cdot SR+0.691(\text{cem/bit})]} \\
 \text{Category D: } N_{PD,FB} &= \frac{1}{30} \cdot 10^{[-1.625+11.938 \cdot RD+0.0726 \cdot PS-1.628 \cdot SR+0.691(\text{cem/bit})]}
 \end{aligned}
 \tag{11}$$

where

$N_{PD,FB}$	= structural capacity (load repetitions)
RD	= relative density (proportion), defined in Section 3.3
PS	= plastic strain (percent)
SR	= stress ratio (proportion), defined in Section 3.4
cem/bit	= ratio of bitumen and cement contents (percent)

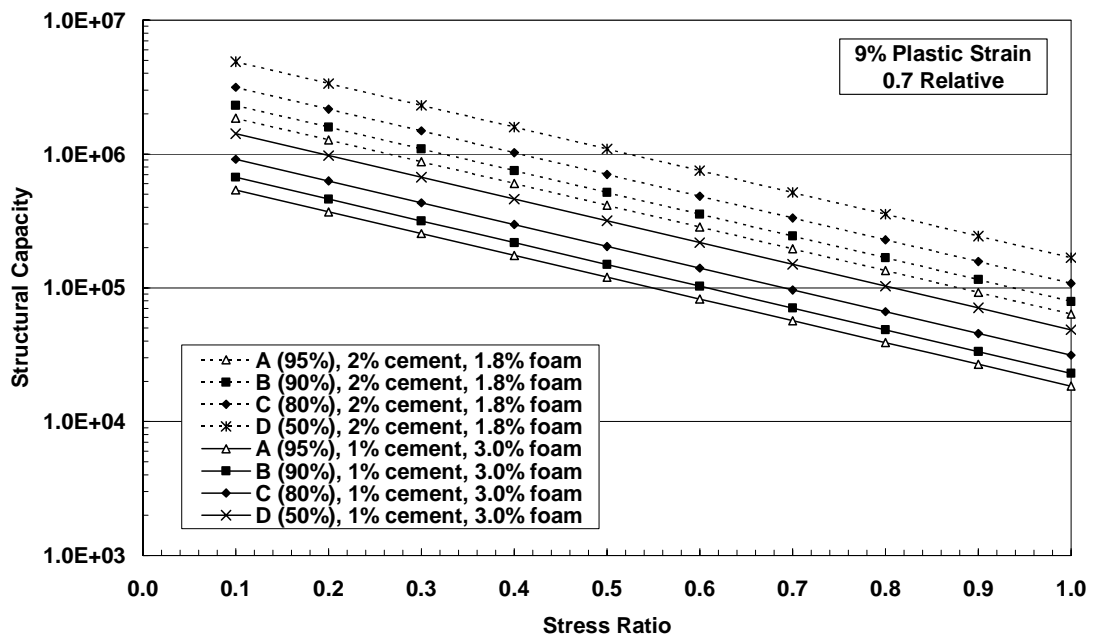


Figure 22. Permanent Deformation Transfer Function

4.4. Effective Fatigue

In this section, a transfer function for the effective fatigue of foamed bitumen treated layers is developed. The function is calibrated from HVS data, mechanistic pavement analyses and laboratory test data.

4.4.1 HVS Effective Fatigue Transfer Function

The back-calculated stiffnesses from the in-depth MDD data discussed in Section 2.4.4 were used to develop an effective fatigue transfer function for the structural design of foamed bitumen treated layers in pavement structures.

From the data in Figure 8 it was noticed that the trend could be separated into three phases: the initial rapid decrease in stiffness; followed by a gradual decrease in stiffness, and finally, a constant stiffness indicative of an equivalent granular state. Not all the test sections had all three phases, particularly at the higher loads where the equivalent granular state was rapidly achieved. Attempts to fit a single curve to describe the reduction in stiffness due to trafficking were unsuccessful.

The time until the beginning of the equivalent granular state is defined as the effective fatigue life. This is reasonable because, at this point, the base layer is in a weakened

state with a reduced stiffness. The condition of the layer in the equivalent granular state is described in Section 2.4.4.

The effective fatigue life was determined from Figure 8 for the 80 kN load case. For the 40 kN load case, a straight line was fitted to the gradually decreasing stiffness data for each MDD, and extrapolated to determine the number of repetitions to a stiffness of 400 MPa. A straight line fit gives a conservative estimate of the repetitions to the equivalent granular state. The results of the effective fatigue life estimates are shown in Figure 23. Also shown in Figure 23 is a trend line determined from the data, the form of which is given in Equation (12).

$$N_{F,FB} = 10^{(a-bWL)} \quad (12)$$

where $N_{F,FB}$ = effective fatigue life (repetitions to 400 MPa stiffness)
 WL = wheel load (kN)
 a, b = regression coefficients

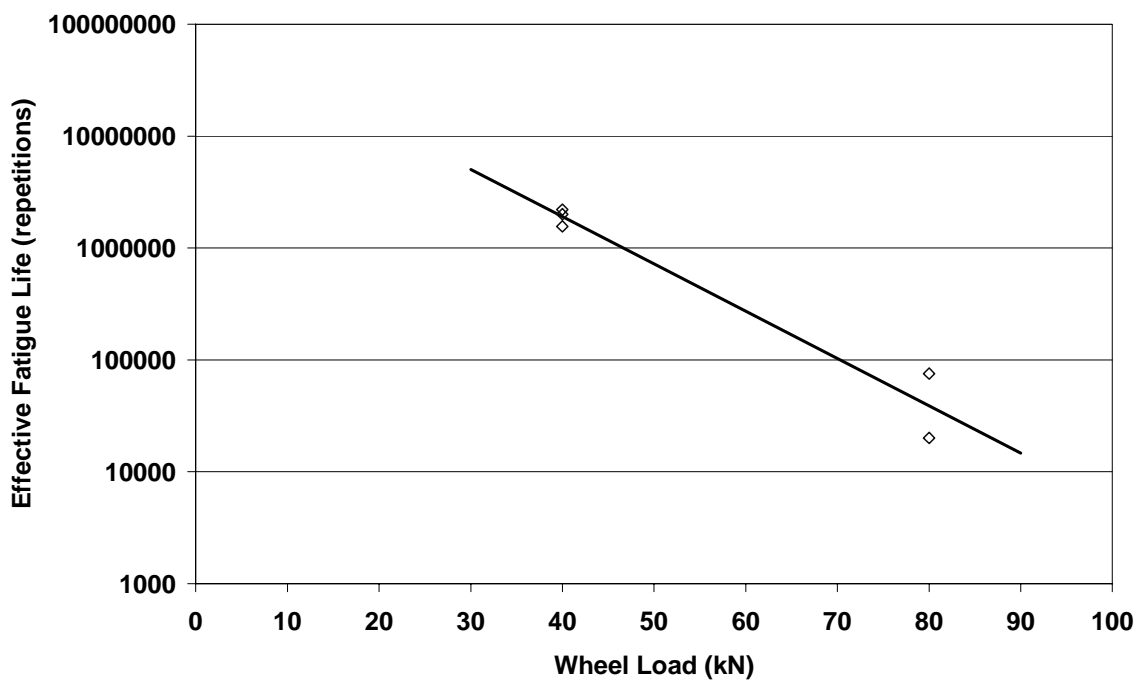


Figure 23. Effective Fatigue Life for Foamed Bitumen Treated Base Material

This model is only valid for this material, with 1.8 percent foamed bitumen and 2 percent cement, the same environmental conditions and pavement structure as at the HVS test sections, and an equivalent granular state stiffness of 400 MPa. For a general pavement design procedure it is necessary to adapt the transfer function to estimate the effective fatigue life using an engineering parameter determined from a mechanistic pavement analysis.

4.4.2 Mechanistic Pavement Analysis for Effective Fatigue

The engineering parameter typically used to relate to the effective fatigue life is the ratio of the tensile strain at the bottom of the pavement layer to the maximum tensile strain that the material can sustain at crack initiation^{7,8}.

Mechanistic analyses, much like that described in Section 4.2.3 for the permanent deformation behaviour, were performed to determine the maximum tensile strain in the pavement. The maximum tensile strain values were obtained for each MDD from each test section. The stiffness values used in the analyses were the initial stiffnesses. Two sets of data were used for each test section. For Section 409A4, the back-calculated stiffnesses of each MDD at 10 and 1000 repetitions were used, for an 80 kN wheel load. For Section 411A4 the stiffnesses of each MDD at 10 and 2000 repetitions were used. The strains were calculated for a 40 kN wheel load. The layer thicknesses were determined from the test pit data. The strain was calculated under and between the wheel at the bottom of the foamed bitumen layer, and the maximum value was used.

4.4.3 Effective Fatigue Transfer Function

Effective fatigue transfer functions for stabilised materials typically relate the ratio of the tensile strain in the pavement to the strain-at-break from a laboratory flexural beam test⁷. This is called the strain ratio.

For the HVS pavement structures the average strain-at-break (ϵ_b) value was determined from the values given in Table 3 for 2 percent cement and 1.8 percent foamed bitumen. Using this value, and the tensile strains (ϵ) from the mechanistic pavement analyses, the strain ratio (ϵ/ϵ_b) was calculated. These data were then used to revise the effective fatigue function in Equation (12), with the strain ratio replacing the wheel load.

The transfer function was adapted to account for the different reliability levels of the different traffic categories. A reliability of 95 percent corresponds to Category A roads, 90 percent to Category B, 80 percent to Category C and 50 percent to Category D roads⁷. The transfer functions are shown in Equation (13) and in Figure 24. The R^2 of the transfer function regression fit is 0.79.

Effective Fatigue Transfer Function:

$$\begin{aligned}
 \text{Category A: } N_{F,FB} &= 10^{\left[6.339 - 0.708\left(\frac{\varepsilon}{\varepsilon_b}\right)\right]} \\
 \text{Category B: } N_{F,FB} &= 10^{\left[6.499 - 0.708\left(\frac{\varepsilon}{\varepsilon_b}\right)\right]} \\
 \text{Category C: } N_{F,FB} &= 10^{\left[6.579 - 0.708\left(\frac{\varepsilon}{\varepsilon_b}\right)\right]} \\
 \text{Category D: } N_{F,FB} &= 10^{\left[6.619 - 0.708\left(\frac{\varepsilon}{\varepsilon_b}\right)\right]}
 \end{aligned}
 \tag{13}$$

where $N_{F,FB}$ = effective fatigue life of foamed bitumen layer
 $\varepsilon/\varepsilon_b$ = strain ratio
 ε = maximum tensile strain at the bottom of the layer
 ε_b = strain-at-break from laboratory testing

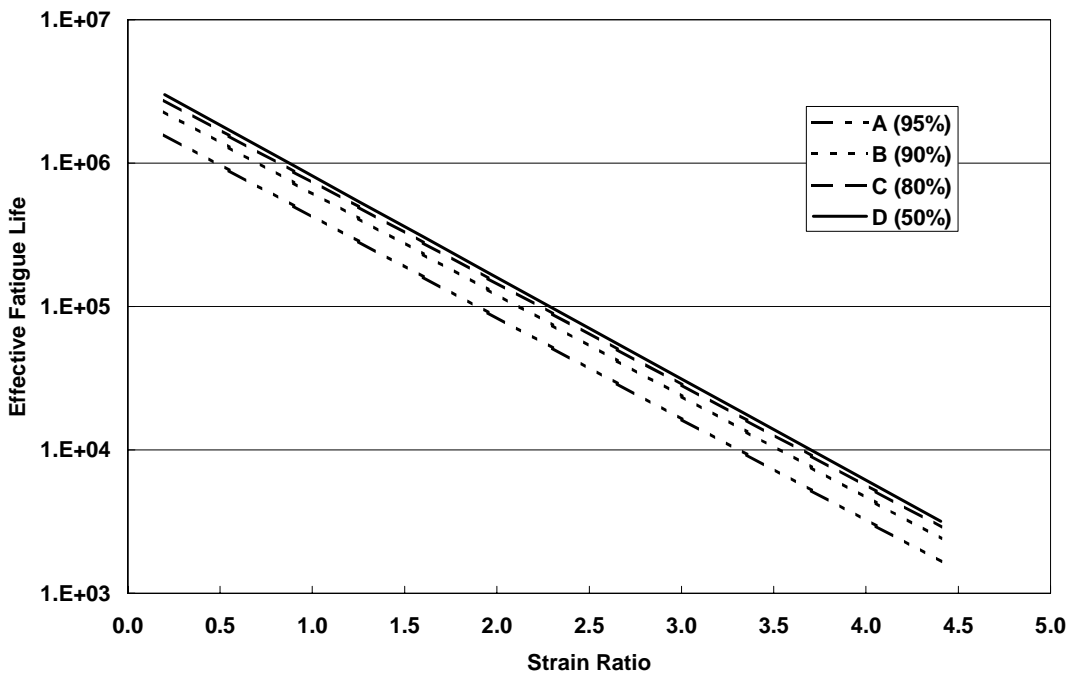


Figure 24. Effective Fatigue Life Transfer Function

This transfer function is developed from the HVS test sections, for a base layer with 2 percent cement and 1.8 percent foamed bitumen. There are no HVS data available to check this effective fatigue function for different combinations of cement and foamed bitumen contents, or to allow incorporation of a cement to bitumen ratio in the transfer function. Figure 13 demonstrated the improved flexibility with an increase in the foamed bitumen content. Because of this, it is expected that the slope of this curve may flatten

with an increase in the foamed bitumen content. Until data are available to confirm this hypothesis and to update the transfer function, the effect of different foamed bitumen and cement contents are only accounted for in the strain-at-break value. Using the transfer function shown in Figure 13, if a higher strain-at-break is determined from a mix tested with an increased foamed bitumen content the strain ratio is reduced and consequently a longer effective fatigue life is obtained.

At low strains, which could result from very thick layers, the strain ratio becomes small, approaching zero. At this stage a constant fatigue life is predicted, which is the intercept of each curve shown in Figure 24. Although the strain ratio may be small, the stiffness of the material will still reduce under traffic. The stress ratio for a pavement with a small tensile strain is also likely to be small, resulting in a long permanent deformation life.

It must be emphasised that the end of the effective fatigue life is not a terminal distress and the pavement is not likely to have failed. After the effective fatigue life, it is assumed that the layer will continue to support loading and will respond as an equivalent granular material. The TRH4⁸ procedure should be followed to analyse the phases of the pavement life. The selection of moduli for the different phases is critical to the analyses, and are recommended in a companion report⁹.

4.4.4 Comparison of Effective Fatigue Life Transfer Functions for Foamed Bitumen and Cemented Materials

A comparison between the effective fatigue lives of cemented and foamed bitumen materials is shown in Figure 25 for Category A and D roads. The transfer function for the cemented material was obtained from Theyse⁷. The effective fatigue lives of the two materials are in the same range, which is expected because of the 2 percent cement in the foamed bitumen mix. The effective fatigue transfer function for the foamed bitumen treated material has a flatter slope than for the cemented materials. This indicates that the foamed bitumen treated material is slightly less sensitive to changes in the strains, and hence to the loads. The foamed bitumen material is therefore slightly less load sensitive.

Although the values are in the same range, the strain-at-break values for the cemented materials are smaller than for the foamed bitumen materials¹. This means that, for pavement structures with cemented and foamed bitumen layers, if the same strain is calculated from the mechanistic pavement analysis, the strain ratio will be lower for the foamed bitumen material, and hence the effective fatigue life will be longer. This is reasonable, as the addition of the foamed bitumen appears to increase the flexibility of the material.

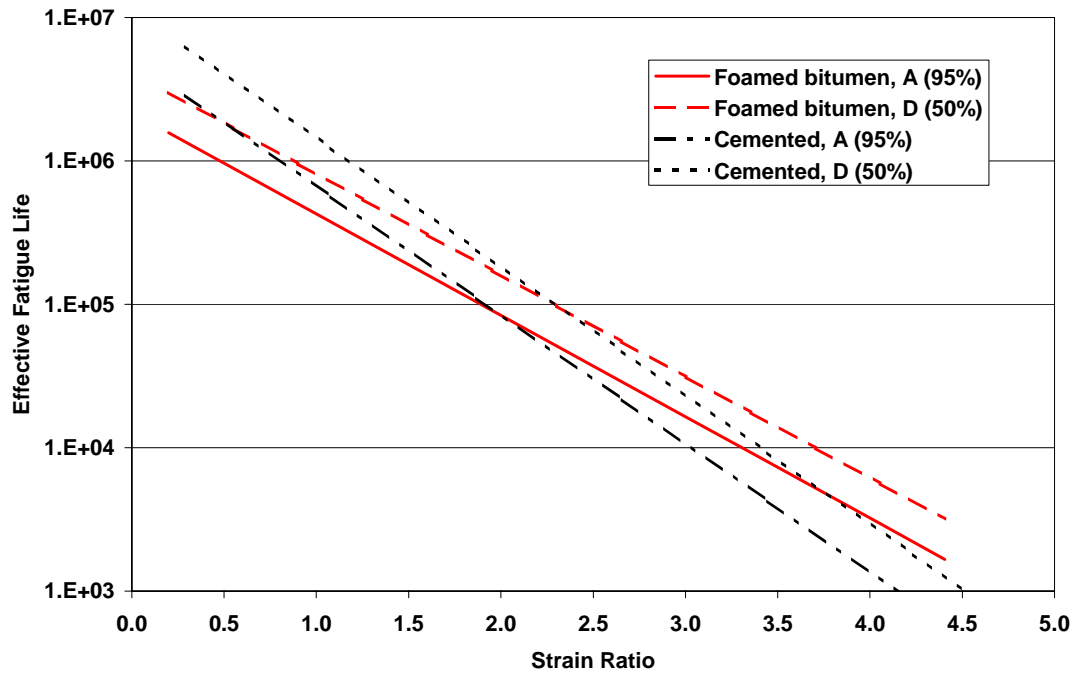


Figure 25. Comparison of Foamed Bitumen and Cemented Materials Effective Fatigue Lives

4.5. Load Sensitivity and Damage Exponents

The HVS data were used to estimate the load sensitivity and damage exponents of foamed bitumen layers. The damage exponents are different for effective fatigue and permanent deformation. The factors are only applicable to the materials and pavement structure of the HVS test sections.

4.5.1 Permanent Deformation

The HVS data can also be used to determine the load sensitivity and damage exponents for these materials. The damage exponent, d , is used in Equation (14) to determine the damage caused by a particular wheel load, relative to the damage caused by a standard wheel load. The damage exponent is then used to convert the traffic for a specific design case, to its equivalent number of standard axle loads.

$$\left(\frac{N_x}{N_{std}} \right) = \left(\frac{P_x}{P_{std}} \right)^d \quad (14)$$

- where N_x = load repetitions at wheel load
 N_{std} = load repetitions at standard wheel load
 P_x = wheel load
 P_{std} = standard wheel load
 d = damage exponent

The damage exponent was calculated by relating the rutting under the 80 kN wheel load to the rutting under the 40 kN wheel load. The 40 kN HVS wheel load is equivalent to an 80 kN standard axle load. For each MDD, the number of load repetitions to 10 percent plastic strain was calculated. This plastic strain value is arbitrary, although the choice of a different value would not significantly affect the results. For the five MDDs, this gave three values for the 40 kN load repetitions and two for the 80 kN load repetitions. Because of the variability in the MDD data on each test section, and because the 40 kN and 80 kN wheel loads were used on two different test sections, all combinations of data were used to calculate the damage exponent. The damage exponents for these combinations are shown in Table 5.

Table 5. Permanent Deformation Damage Exponents for Combinations of MDDs and Test Sections

		40 kN Wheel load (Section 411A4)		
		MDD 4	MDD 8	MDD 12
80 kN Wheel load (Section 409A4)	MDD 4	2.0	3.3	3.8
	MDD 12	0.6	1.9	2.5
<i>Average</i>		2.4		
<i>Standard deviation</i>		1.1		

The range in damage exponents is fairly large. However, this is reasonable given the range in the MDD data. A damage exponent of approximately 2 is expected for these types of materials so this result is reasonable¹⁰. In pavement design a damage exponent of 4 is often assumed, which would result in significant errors in the conversion of the actual traffic to the design traffic for a specific design case. These errors are conservative.

4.5.2 Effective Fatigue

The effective fatigue life data were used to estimate a damage exponent for foamed bitumen treated materials. It was noticed that the foamed bitumen treated material is load sensitive, with the higher loads causing a more rapid deterioration in the stiffness. The damage exponent relates the relative difference in damage between the 40 and 80 kN wheel loads.

The damage exponent was calculated from the effective fatigue life for all the MDDs on Sections 409A4 and 411A4, using Equation (14). The 100 kN and 80 kN data for Sections 409A4/B4 and 411A4, respectively, were ignored, because of their load history. The damage exponents are given in Table 6. The difference between the values for MDD4 and MDD12 of Section 409A4 is because of the large difference in the number of repetitions to reach the equivalent granular state, 20000 and 75000 load repetitions, respectively.

Table 6. Effective Fatigue Damage Exponents for Combinations of MDDs and Test Sections

		40 kN Wheel load (Section 411A4)		
		MDD 4	MDD 8	MDD 12
80 kN Wheel load (Section 409A4)	MDD 4	6.6	6.3	6.8
	MDD 12	4.7	4.4	4.8
<i>Average</i>		5.6		
<i>Standard deviation</i>		1.1		

The damage exponent for effective fatigue is considerably higher than for permanent deformation, which is expected. Again, assuming a value of 4 or 4.2 would introduce errors but, in this case, non-conservative errors. It must be emphasised that these damage exponents are calculated from the observed behaviour of one material in one pavement structure for one environmental condition, and should therefore be used with caution for other materials, pavement structures or environmental conditions.

5. CONCLUSIONS

This report described the development of structural design models for foamed bitumen treated materials for incorporation into the South African Mechanistic-Empirical Design Procedure. The models were developed from the HVS data and calibrated and expanded to a wider range of pavement and material conditions using laboratory data.

The HVS test sections include a foamed bitumen treated milled ferricrete with 2 percent cement and 1.8 percent foamed bitumen. A wider range of foamed bitumen and cement contents were tested in various laboratory tests. The structural design models (transfer functions) were developed from the available data and are therefore most applicable to situations with similar cement and foamed bitumen contents. The models will be calibrated, modified and updated as more data become available. At this stage, no other mechanistic-empirical structural design models are available for foamed bitumen treated materials.

The laboratory tests showed that foamed bitumen improves the flexibility and therefore the fatigue resistance of the material, with higher foamed bitumen contents showing higher flexibility. However, with the addition of cement, a minimum amount of foamed bitumen is necessary to affect the flexibility. The cement improves the compressive strength and therefore the permanent deformation resistance of the material. The optimum balance between the cement and foamed bitumen contents depends on the desired material properties.

Preliminary structural performance models for the foamed bitumen treated material were determined from the HVS data, both for permanent deformation and for effective fatigue. The models determine the number of load repetitions to the selected failure criteria as a function of the wheel load. Using the laboratory data and mechanistic pavement analyses, these models were converted to determine the structural capacity or effective fatigue life as a function of an engineering parameter. The stress ratio was used for permanent deformation and the strain ratio was used for effective fatigue.

The permanent deformation transfer function was determined from dynamic triaxial tests over a range of relative densities and stress ratios to various levels of plastic strain for two combinations of foamed bitumen and cement. This model was calibrated with the permanent deformation response observed on the HVS site. The transfer function accounts for the different road categories, Category A to D. The permanent deformation

model is given in Section 4.3.2 in Equation (11) and Figure 22. The model includes a term for the ratio of the cement to foamed bitumen content.

The effective fatigue transfer function predicts the expected pavement life to reach an equivalent granular state. Back-calculated elastic stiffnesses from the HVS sections showed that the stiffness of the foamed bitumen treated material (2 percent cement, 1.8 percent foamed bitumen) initially decreased rapidly, thereafter with a more gradual decrease to an equivalent granular state (Figure 8). This gradual decrease is load dependent. Regardless of the load, an equivalent granular state was reached at approximately 400 MPa. The transfer function determines the effective fatigue life, which is the pavement life to reach the equivalent granular state. The equivalent granular state does not imply the pavement has reached a terminal failure condition, rather that the end of this phase of the pavement life has been achieved. The transfer function for effective fatigue is given in Section 4.4.3, Equation (13) and Figure 24.

Both the permanent deformation and effective fatigue transfer functions capture the increasing flexibility, and therefore effective fatigue life, with increasing foamed bitumen contents; and the increasing compressive strength, and therefore permanent deformation resistance, of increasing the cement content.

Using the HVS data, damage exponents were estimated for both effective fatigue and permanent deformation for the specific foamed bitumen treated material. The damage exponent for permanent deformation is approximately 2.4, which is significantly lower than the 4 or 4.2 values typically assumed. The effective fatigue damage exponent is however, larger, approximately 5.6. This shows that the effective fatigue response of the test section is much more load sensitive than the permanent deformation response, and using the assumed values for effective fatigue analyses would result in a non-conservative error in pavement design and analyses.

6. REFERENCES

1. Long, F.M. and H.L.Theyse, *Laboratory Testing for the HVS Sections on Road P243/1*, Transportek, CSIR, Contract Report CR-2001/22, 2001.
2. Semmelink, C.J, and P.B Botha, *Evaluation of Foam Bitumen and Emulsion Treated Ferricrete Material on the New HVS Site in the Initial Stages*, Transportek, CSIR, LR2000/1/JR3879, 2001.
3. Steyn, W.J.vdM., *Level one data analysis of HVS tests on Foam Treated Gravel and Emulsion Treated Gravel on Road P243-1: 80 kN and 100 kN test sections*, Transportek, CSIR, Contract Report CR-2001/5, 2001.
4. Mancotywa, W.S., *First Level Analysis Report: 2nd phase HVS Testing of the Emulsion Treated Gravel and Foam Treated Gravel Base Sections on Road P243/1 near Vereeniging*, Transportek, CSIR, Contract Report CR-2001/53, 2001.
5. Robroch, S., *Laboratory Testing on Foamed Bitumen and Cement Treated Materials from the HVS Test Sections on Road P243/1*, Transportek, CSIR, Contract Report, CR-2001/69, 2001.
6. Theyse, H.L., The development of mechanistic-empirical permanent deformation design models for unbound pavement materials from laboratory and accelerated pavement test data, *Proceedings of the Fifth International Symposium on Unbound Aggregates in Roads*, Nottingham, 2000.
7. Theyse, H.L., *Overview of the South African Mechanistic Pavement Design Method*, South African Transport Conference, July 2000.
8. Technical Recommendations for Highways, TRH4: *Structural Design of Flexible Pavements for Interurban and Rural Roads*, Draft, Department of Transport, 1996.
9. Long, F.M., *The development of a pavement design catalogue with foamed bitumen treated bases*, Transportek, CSIR, Contract Report CR-2002/09, 2002.
10. Mancotywa, W.S., *Phase 1 testing of experimental sections on Road 2388 near Cullinan*, Transportek, CSIR, Contract Report CR-99/011, 1999.